γ-secretase inhibitors directed to the active site covalently label presenilin 1. Nature 405:689–694.

Loo TW, Clarke DM (2001a) Cross-linking of human multidrug resistance P-glycoprotein by the substrate, tris-(2-maleimidoethyl)amine, is altered by ATP hydrolysis. Evidence for rotation of a transmembrane helix. J Biol Chem 276:31800–31805.

Loo TW, Clarke DM (2001b) Determining the dimensions of the drug-binding domain of human P-glycoprotein using thiol cross-linking compounds as molecular rulers. J Biol Chem 276:36877–36880.

Micchelli CA, Esler WP, Kimberly WT, Jack C, Berezovska O, Kornilova A, Hyman BT, Perrimon N, Wolfe MS (2003) γ-Secretase/presenilin inhibitors for Alzheimer's disease phenocopy Notch mutations in *Drosophila*. FASEB J 17:79–81.

Morohashi Y, Kan T, Tominari Y, Fuwa H, Okamura Y, Watanabe N, Sato C, Natsugari H, Fukuyama T, Iwatsubo T, Tomita T (2006) C-terminal fragment of presenilin is the molecular target of a dipeptidic γ-secretase-specific inhibitor DAPT (*N*-[*N*-(3,5-difluorophenacetyl)-L-alanyl]-*S*-phenylglycine *t*-butyl ester). J Biol Chem 281:14670–14676.

Nakaya Y, Yamane T, Shiraishi H, Wang HQ, Matsubara E, Sato T, Dolios G, Wang R, De Strooper B, Shoji M, Komano H, Yanagisawa K, Ihara Y, Fraser P, St George-Hyslop P, Nishimura M (2005) Random mutagenesis of presenilin-1 identifies novel mutants exclusively generating long amyloid beta-peptides. J Biol Chem 280:19070–19077.

Ogura T, Mio K, Hayashi I, Miyashita H, Fukuda R, Kopan R, Kodama T, Hamakubo T, Iwastubo T, Tomita T, Sato C (2006) Three-dimensional structure of the γ-secretase complex. Biochem Biophys Res Commun 343:525–534.

Oh YS, Turner RJ (2005) Evidence that the COOH terminus of human presenilin 1 is located in extracytoplasmic space. Am J Physiol Cell Physiol 289:C576–C581.

Sato C, Morohashi Y, Tomita T, Iwatsubo T (2006) Structure of the catalytic pore of γ-secretase probed by the accessibility of substituted cysteines. J Neurosci 26:12081–12088.

Selkoe DJ, Wolfe MS (2007) Presenilin: running with scissors in the membrane. Cell 131:215–221.

Shearman MS, Beher D, Clarke EE, Lewis HD, Harrison T, Hunt P, Nadin A, Smith AL, Stevenson G, Castro JL (2000) L-685,458, an aspartyl protease transition state mimic, is a potent inhibitor of amyloid β-protein precursor γ-secretase activity. Biochemistry 39:8698–8704.

Spasic D, Tolia A, Dillen K, Baert V, De Strooper B, Vrijens S, Annaert W (2006) Presenilin-1 maintains a nine-transmembrane topology throughout the secretory pathway. J Biol Chem 281:26569–26577.

Steiner H, Romig H, Pesold B, Philipp U, Baader M, Citron M, Loetscher H, Jacobsen H, Haass C (1999) Amyloidogenic function of the Alzheimer's disease-associated presenilin 1 in the absence of endoproteolysis. Biochemistry 38:14600–14605.

Takasugi N, Tomita T, Hayashi I, Tsuruoka M, Niimura M, Takahashi Y, Thinakaran G, Iwatsubo T (2003) The role of presenilin cofactors in the γ-secretase complex. Nature 422:438–441.

Thinakaran G, Regard JB, Bouton CM, Harris CL, Price DL, Borchelt DR, Sisodia SS (1998) Stable association of presenilin derivatives and absence of presenilin interactions with APP. Neurobiol Dis 4:438–453.

Tian G, Ghanekar SV, Aharony D, Shenvi AB, Jacobs RT, Liu X, Greenberg BD (2003) The mechanism of γ-secretase: multiple inhibitor binding sites for transition state analogs and small molecule inhibitors. J Biol Chem 278:28968–28975.

Tolia A, Chávez-Gutiérrez L, De Strooper B (2006) Contribution of presenilin transmembrane domains 6 and 7 to a water-containing cavity in the γ-secretase complex. J Biol Chem 281:27633–27642.

Tomita T, Iwatsubo T (2006) γ-Secretase as a therapeutic target for treatment of Alzheimer's disease. Curr Pharm Des 12:661–670.

Tomita T, Maruyama K, Saido TC, Kume H, Shinozaki K, Tokuhiro S, Capell A, Walter J, Grünberg J, Haass C, Iwatsubo T, Obata K (1997) The presenilin 2 mutation (N141I) linked to familial Alzheimer disease (Volga German families) increases the secretion of amyloid β protein ending at the 42nd (or 43rd) residue. Proc Natl Acad Sci USA 94:2025–2030.

Tomita T, Takikawa R, Koyama A, Morohashi Y, Takasugi N, Saido TC, Maruyama K, Iwatsubo T (1999) C terminus of presenilin is required for overproduction of amyloidogenic Aβ42 through stabilization and endoproteolysis of presenilin. J Neurosci 19:10627–10634.

Tomita T, Watabiki T, Takikawa R, Morohashi Y, Takasugi N, Kopan R, De Strooper B, Iwatsubo T (2001) The first proline of PALP motif at the C terminus of presenilins is obligatory for stabilization, complex formation, and γ-secretase activities of presenilins. J Biol Chem 276:33273–33281.

Ulmschneider MB, Sansom MS (2001) Amino acid distributions in integral membrane protein structures. Biochim Biophys Acta 1512:1–14.

von Heijne G (1991) Proline kinks in transmembrane α-helices. J Mol Biol 218:499–503.

Wang J, Brunkan AL, Hecimovic S, Walker E, Goate A (2004) Conserved "PAL" sequence in presenilins is essential for γ-secretase activity, but not required for formation or stabilization of γ-secretase complexes. Neurobiol Dis 15:654–666.

Wang J, Beher D, Nyborg AC, Shearman MS, Golde TE, Goate A (2006) C-terminal PAL motif of presenilin and presenilin homologues required for normal active site conformation. J Neurochem 96:218–227.

Wang Y, Zhang Y, Ha Y (2006) Crystal structure of a rhomboid family intramembrane protease. Nature 444:179–180.

Watanabe N, Tomita T, Sato C, Kitamura T, Morohashi Y, Iwatsubo T (2005) Pen-2 is incorporated into the γ-secretase complex through binding to transmembrane domain 4 of presenilin 1. J Biol Chem 280:41967–41975.

Wolfe MS, Kopan R (2004) Intramembrane proteolysis: theme and variations. Science 305:1119–1123.

Wu Z, Yan N, Feng L, Oberstein A, Yan H, Baker RP, Gu L, Jeffrey PD, Urban S, Shi Y (2006) Structural analysis of a rhomboid family intramembrane protease reveals a gating mechanism for substrate entry. Nat Struct Mol Biol 13:1084–1091.

Expert Opinion

Peptides inhibiting specific cleaving activities of presenilins

WO2004026331

Taisuke Tomita

The University of Tokyo, Graduate School of Pharmaceutical Sciences, Department of Neuropathology and Neuroscience, Hongo 7-3-1, Bunkyo, Tokyo 113-0033, Japan

Genetic and biological studies provide evidence that the deposition of amyloid-β peptide contributes to the etiology of Alzheimer's disease (AD). Amyloid-β peptides are generated from amyloid-β precursor protein by β- and γ-secretases that are plausible molecular targets for AD treatment. γ-Secretase is an intramembrane-cleaving aspartic protease that is composed of a membrane protein complex containing presenilin. This patent describes a method to inhibit γ-secretase-mediated cleavage by new cell-permeable peptides that are designed on the basis of the interaction mode of amyloid-β precursor protein and presenilin. This patent provides a new strategy for the modulation of the γ-secretase activity towards the development of AD therapeutics.

Keywords: Alzheimer's disease, amyloid-β peptide, amyloid-β precursor protein, γ-secretase, presenilin

Expert Opin. Ther. Patents (2008) 18(9):1097-1100

1. Introduction

Alzheimer's disease (AD) is a progressive demential neurodegenerative disorder characterized pathologically by the presence of senile plaques and neurofibrillary changes in the brains of affected individuals [1,2]. Senile plaques are composed of amyloid-β peptides (Aβ) that are proteolytically produced from amyloid-β precursor protein (APP). These precursor proteins are initially cleaved by β-secretase to generate a 99-residue C-terminal fragment (*C*99) that is then cleaved by γ-secretase within transmembrane domain (TMD) to generate Aβ (**Figure 1**) [2,3]. C-terminal length of Aβ generated by γ-secretase is heterogeneous; Aβ42 is the initially and predominantly deposited peptide in the brains of AD patients and aggregates much faster than the predominant Aβ40 species, whereas the levels of secreted Aβ42 are relatively minor. Genetic mutations in APP, presenilin (PS) 1 and PS2 genes that cosegregate with familial AD (FAD) cases specifically increase the Aβ42 production [3-5]. These data strongly implicate that the production, the aggregation and the deposition of Aβ in brains link to the pathogenesis of AD ('Amyloid Hypothesis') [1,2]. Thus, the modulation of the Aβ levels might provide a disease-modifying therapy against AD on the basis of its etiology, and γ-secretase is one of the plausible molecular targets.

Several lines of evidence indicate that γ-secretase is a membrane protein complex consisting of PS, Nicastrin, Aph-1 and Pen-2 [3-5]. Genetic ablation of any of these components resulted in the loss of proteolytic activity, suggesting essential roles of these four proteins in γ-secretase activity. Moreover, the knockout of γ-secretase genes in animals causes developmental abnormalities that are similar to Notch-deficient phenotype. Notch signaling is mediated by the liberation of the Notch intracellular domain (NICD) from the membrane-tethered precursor by intramembrane site-3 (S3) cleavage [6]. NICD traverses to the nucleus where it is

informa
healthcare

10.1517/13543770802327136 © 2008 Informa UK Ltd ISSN 1354-3776

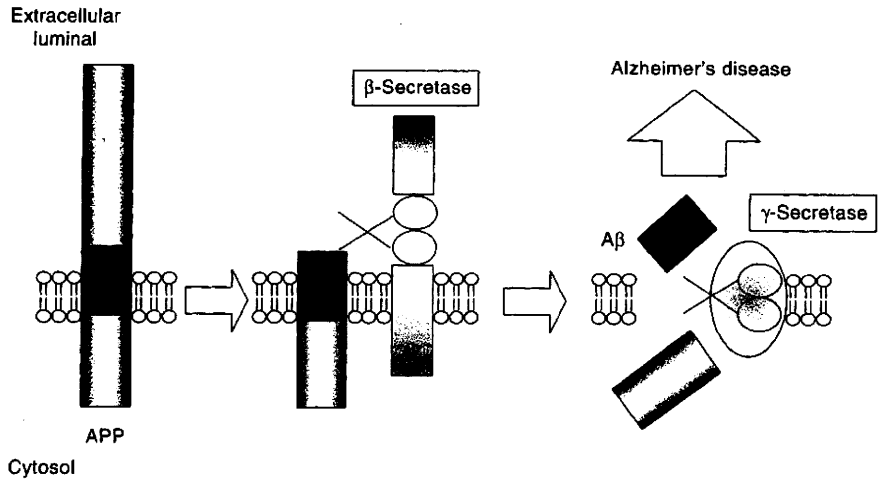

Figure 1. Schematic depiction of APP processing. APP is first shed by β-secretase in the luminal side to generate C99, which is a direct substrate for γ-secretase. γ-Secretase cleavage occurs within the transmembrane region to release Aβ and the intracellular domain.
Aβ: Amyloid-β peptides; APP: Amyloid-β precursor protein.

involved in the regulation of gene transcription. S3 cleavage requires PS and is blocked by γ-secretase inhibitors. So far, extra substrates for γ-secretase-mediated intramembrane proteolysis have been identified, including Notch ligands (i.e., Delta, Jagged), ErbB-4, cadherins, CD44, LRP, Nectin-1α, p75 receptor and syndecan-3 [7]. Thus, simple inhibition of γ-secretase activity causes significant adverse effects. In fact, oral application of a potent γ-secretase inhibitor (i.e., compound E or LY-411,575) causes gastrointestinal toxicity and atrophy of the thymus [8-10]. Thus, in view of these side effects caused by blockade of Notch signaling, there is a compelling need for the development of inhibitors that can selectively inhibit APP cleavage but not the other substrates including Notch.

2. Chemistry

The inventors synthesized peptides by the conventional method. Cell permeability and membrane anchoring of these peptides were achieved by the addition of transport peptide (TP) [11,12] and palmitoyl group, respectively.

3. Biology and action

Presenilin harbors two catalytic aspartates within TMDs 6 and 7 [5,13], and serves as the active center of γ-secretase complex with a 'catalytic pore' structure [14-16]. However, pharmacological studies implicate that γ-secretase harbors 'substrate binding site' other than the catalytic site [17-19]. The inventors have previously reported that the C terminus and the first TMD of PS1 directly bound the TMD of APP [20,21]. To develop the new method to inhibit/modulate the γ-secretase activity, the inventors examined the effect of several synthetic peptides mimicking the binding domain in PS1 or APP on the production of Aβ peptides using *in vitro* assay (**Figure 2**). They found that the TP-fused peptides corresponding to the C terminus of PS1 (e.g., A5; TP-FMDQLAFHQFYI) or the APP TMD (e.g., D7; VVIATVIVITLVMLK-TP) significantly decreased the Aβ generation. Familial AD-linked mutations at 717-position in the APP sequence, which are known as Aβ42-overproducing mutations [22,23], increased the inhibitory effect of the synthetic peptides (e.g., AA9; VVIATVIIITLVMLKKKQ-TP). Moreover, extension of both N- and C-terminal sides of the binding domain in the APP-mimicking peptides (e.g., AA4; VVIATVIVITLVMLKKKQ-TP, DD3; MVGGVVIATVIVITLVMLKKKQ-TP) also significantly increased the inhibitory potency *in vitro*. Then the inventors tested the effect of the APP-mimicking peptide D7 in cell-based luciferase assay [24]. D7 significantly decreased the γ-secretase-mediated cleavage of APP but not Notch, suggesting that it acts as an APP-specific γ-secretase inhibitor. Finally, to study the mode of action of the inhibitory peptides, pull-down assay using biotinylated inhibitory peptide was performed. The APP-mimicking peptide specifically bound the APP holoprotein as well as PS1 polypeptides. Intriguingly, the binding of the peptide and APP was observed in PS1/2 double knockout cells in which γ-secretase was diminished [25], suggesting that these peptides directly targeted APP itself irrespective of the formation of functional γ-secretase complex. These data suggest that the inhibitory effect of the peptides was accomplished by interference in the interaction between APP and PS1. Collectively, this invention indicates that i) the TP-fused peptides corresponding to the C terminus of PS1 as well as the TMD of APP have an inhibitory effect on the proteolytic

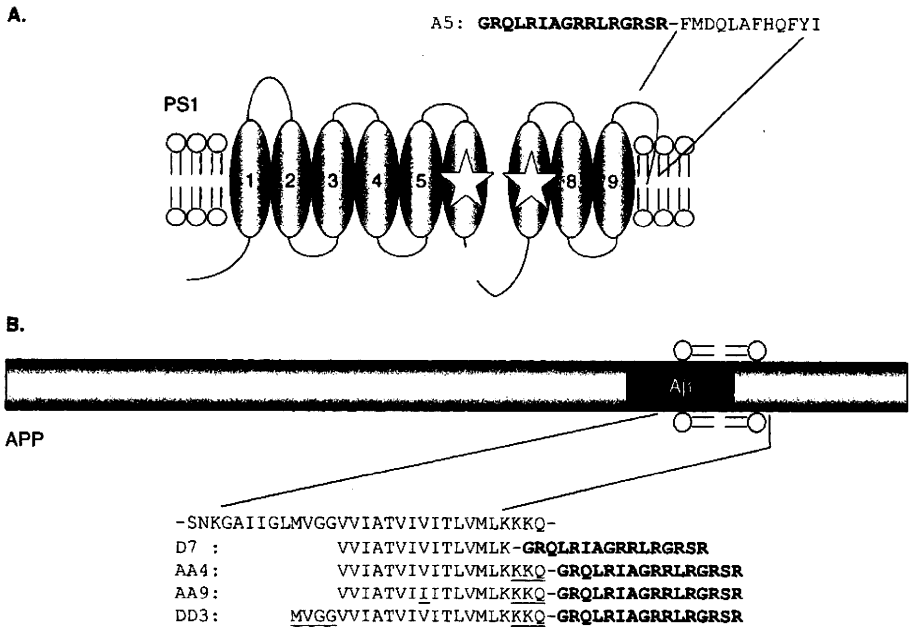

Figure 2. Examples of the inhibitory peptides described in this invention. A. Schematic depiction of PS1 and the location of amino acid sequence corresponding to the inhibitory peptide A5. Transport peptide is indicated in bold. **B.** Schematic depiction of APP and the amino acid sequences of the inhibitory peptides. Different residues in the peptides compared to D7 are indicated using underline.
Aβ: Amyloid-β peptides; APP: Amyloid-β precursor protein; PS1: Presenilin 1.

activity of γ-secretase complex; ii) the inhibitory peptides are able to act on the γ-secretase in intact cultured cells; and iii) the APP-mimicking peptide specifically inhibits the APP-cleaving γ-secretase activity by interfering in the enzyme–substrate interaction.

4. Expert opinion

According to the Amyloid Hypothesis, amyloid-targeting strategy might provide an etiology-based disease-modifying therapy against AD [1-5]. However, the inhibition of γ-secretase, the essential enzyme for the Aβ production, causes adverse effects by the inhibition of Notch signaling. Thus, the development of methods to specifically modulate APP-cleaving γ-secretase activity is now one of the compelling needs for AD therapeutics. As no structural data of γ-secretase complex at high resolution has been available [5], the molecular mechanism whereby γ-secretase cleaves its substrate still remains unknown. Especially, understanding the molecular action of the substrate recognition system in γ-secretase complex would pave the road for the substrate-specific drug development. In this context, the invention disclosed here contains a new approach for the modulation of enzymatic activity. The APP-mimicking peptide specifically inhibits the APP-cleaving γ-secretase activity through a direct interaction with APP. It is noteworthy that the inventors disclosed the possible mode of action of the inhibitory peptide. Thus, although a peptide-based drug design and development is still difficult, this patent suggests an important direction for AD therapeutic development – a strategy to target substrate itself (i.e., APP). In fact, some compounds including γ-secretase modulators have been recently revealed as 'substrate-targeting' compounds [26,27]. Moreover, the amino acid sequence of APP used in this patent contains ε-cleavage site that is known as a putative first cleavage in γ-secretase-mediated proteolysis [28-31]. Several FAD-linked as well as artificial mutations in this sequence increase the generation of Aβ42, supporting the notion that this region is important for the recognition and the cleavage by γ-secretase [22,23,32,33]. Thus, the peptides disclosed here may also be applicable for the chemical biological approach to analyzing the enzymatic characteristics of γ-secretase. Nevertheless, further challenges to identify small compounds targeting the substrate itself or the substrate recognition system in the γ-secretase complex would provide not only a new aspect of γ-secretase-mediated cleavage but also effective AD therapeutics without severe adverse effects.

Declaration of interest

The author states no conflict of interest and has received no payment in preparation of this manuscript.

Bibliography

1. Wolfe MS. Shutting down Alzheimer's. Sci Am 2006;294(5):72-9
2. Haass C, Selkoe DJ. Soluble protein oligomers in neurodegeneration: lessons from the Alzheimer's amyloid beta-peptide. Nat Rev Mol Cell Biol 2007;8(2):101-12
3. Tomita T, Iwatsubo T. Gamma-secretase as a therapeutic target for treatment of Alzheimer's disease. Curr Pharm Des 2006;12(6):661-70
4. Tomita T. At the frontline of Alzheimer's disease treatment: gamma-secretase inhibitor/modulator mechanism. Naunyn Schmiedebergs Arch Pharmacol 2008;377(4-6):70-8
5. Selkoe DJ, Wolfe MS. Presenilin: running with scissors in the membrane. Cell 2007;131(2):215-21
6. Ilagan MX, Kopan R. SnapShot: notch signaling pathway. Cell 2007;128(6):1246
7. Parks AL, Curtis D. Presenilin diversifies its portfolio. Trends Genet 2007;23(3):140-50
8. Searfoss GH, Jordan WH, Calligaro DO, et al. Adipsin, a biomarker of gastrointestinal toxicity mediated by a functional gamma-secretase inhibitor. J Biol Chem 2003;278(46):46107-16
9. Wong GT, Manfra D, Poulet FM, et al. Chronic treatment with the gamma-secretase inhibitor LY-411,575 inhibits beta-amyloid peptide production and alters lymphopoiesis and intestinal cell differentiation. J Biol Chem 2004;279(13):12876-82
10. Milano J, McKay J, Dagenais C, et al. Modulation of notch processing by gamma-secretase inhibitors causes intestinal goblet cell metaplasia and induction of genes known to specify gut secretory lineage differentiation. Toxicol Sci 2004;82(1):341-58
11. Langedijk JP. Transport peptides among which C-terminal Erns peptide and analogues thereof. WO0200882; 2002
12. Langedijk JP. Translocation activity of C-terminal domain of pestivirus Erns and ribotoxin L3 loop. J Biol Chem 2002;277(7):5308-14
13. Wolfe MS, Xia W, Ostaszewski BL, et al. Two transmembrane aspartates in presenilin-1 required for presenilin endoproteolysis and gamma-secretase activity. Nature 1999;398(6727):513-7
14. Li YM, Xu M, Lai MT, et al. Photoactivated gamma-secretase inhibitors directed to the active site covalently label presenilin 1. Nature 2000;405(6787):689-94
15. Tolia A, Chavez-Gutierrez L, De Strooper B. Contribution of presenilin transmembrane domains 6 and 7 to a water-containing cavity in the gamma-secretase complex. J Biol Chem 2006;281(37):27633-42
16. Sato C, Morohashi Y, Tomita T, Iwatsubo T. Structure of the catalytic pore of gamma-secretase probed by the accessibility of substituted cysteines. J Neurosci 2006;26(46):12081-8
17. Tian G, Sobotka-Briner CD, Zysk J, et al. Linear non-competitive inhibition of solubilized human gamma-secretase by pepstatin A methylester, L685458, sulfonamides, and benzodiazepines. J Biol Chem 2002;277(35):31499-505
18. Tian G, Ghanekar SV, Aharony D, et al. The mechanism of gamma-secretase: multiple inhibitor binding sites for transition state analogs and small molecule inhibitors. J Biol Chem 2003;278(31):28968-75
19. Kornilova AY, Bihel F, Das C, Wolfe MS. The initial substrate-binding site of gamma-secretase is located on presenilin near the active site. Proc Natl Acad Sci USA 2005;102(9):3230-5
20. Annaert WG, Esselens C, Baert V, et al. Interaction with telencephalin and the amyloid precursor protein predicts a ring structure for presenilins. Neuron 2001;32(4):579-89
21. Esselens C, Oorschot V, Baert V, et al. Presenilin 1 mediates the turnover of telencephalin in hippocampal neurons via an autophagic degradative pathway. J Cell Biol 2004;166(7):1041-54
22. Suzuki N, Cheung TT, Cai XD, et al. An increased percentage of long amyloid beta protein secreted by familial amyloid beta protein precursor (beta APP717) mutants. Science 1994;264(5163):1336-40
23. Maruyama K, Tomita T, Shinozaki K, et al. Familial Alzheimer's disease-linked mutations at Val717 of amyloid precursor protein are specific for the increased secretion of A beta 42(43). Biochem Biophys Res Commun 1996;227(3):730-5
24. Karlstrom H, Bergman A, Lendahl U, et al. A sensitive and quantitative assay for measuring cleavage of presenilin substrates. J Biol Chem 2002;277(9):6763-6
25. Herreman A, Serneels L, Annaert W, et al. Total inactivation of gamma-secretase activity in presenilin-deficient embryonic stem cells. Nat Cell Biol 2000;2(7):461-2
26. Espeseth AS, Xu M, Huang Q, et al. Compounds that bind APP and inhibit Abeta processing in vitro suggest a novel approach to Alzheimer disease therapeutics. J Biol Chem 2005;280(18):17792-7
27. Kukar TL, Ladd TB, Bann MA, et al. Substrate-targeting gamma-secretase modulators. Nature 2008;453(7197):925-9
28. Sato T, Dohmae N, Qi Y, et al. Potential link between amyloid beta-protein 42 and C-terminal fragment gamma 49-99 of beta-amyloid precursor protein. J Biol Chem 2003;278(27):24294-301
29. Zhao G, Mao G, Tan J, et al. Identification of a new presenilin-dependent zeta-cleavage site within the transmembrane domain of amyloid precursor protein. J Biol Chem 2004;279(49):50647-50
30. Qi-Takahara Y, Morishima-Kawashima M, Tanimura Y, et al. Longer forms of amyloid beta protein: implications for the mechanism of intramembrane cleavage by gamma-secretase. J Neurosci 2005;25(2):436-45
31. Zhao G, Cui MZ, Mao G, et al. Gamma-cleavage is dependent on zeta-cleavage during the proteolytic processing of amyloid precursor protein within its transmembrane domain. J Biol Chem 2005;280(45):37689-97
32. Lichtenthaler SF, Wang R, Grimm H, et al. Mechanism of the cleavage specificity of Alzheimer's disease gamma-secretase identified by phenylalanine-scanning mutagenesis of the transmembrane domain of the amyloid precursor protein. Proc Natl Acad Sci USA 1999;96(6):3053-8
33. Sato T, Tanimura Y, Hirotani N, et al. Blocking the cleavage at midportion between gamma- and epsilon-sites remarkably suppresses the generation of amyloid beta-protein. FEBS Lett 2005;579(13):2907-12

Affiliation

Taisuke Tomita PhD
The University of Tokyo,
Graduate School of Pharmaceutical Sciences,
Department of Neuropathology and Neuroscience,
Hongo 7-3-1, Bunkyo,
Tokyo 113-0033, Japan
Tel: +81 3 5841 4868; Fax: +81 3 5841 4708;
E-mail: taisuke@mol.f.u-tokyo.ac.jp

Altered Function of Factor I Caused by Amyloid β: Implication for Pathogenesis of Age-Related Macular Degeneration from Drusen[1]

Jiying Wang,* Kyoko Ohno-Matsui,[2]* Takeshi Yoshida,* Ariko Kojima,* Noriaki Shimada,* Ken-ichi Nakahama,† Olga Safranova,† Nobuhisa Iwata,‡ Takaomi C. Saido,‡ Manabu Mochizuki,* and Ikuo Morita†

The results of recent studies have implicated local inflammation and complement activation as the processes involved in the pathogenesis of age-related macular degeneration (AMD). We have demonstrated that amyloid β (Aβ), which is deposited in drusen, causes an imbalance in the angiogenesis-related factors in retinal pigment epithelial cells. We have also shown that neprilysin gene-disrupted mice accumulate Aβ, and develop several features of AMD. The purpose of this study was to investigate the mechanisms involved in the development of AMD that are triggered by Aβ. Our results showed that Aβ binds to complement factor I which inhibits the ability of factor I to cleave C3b to inactivated iC3b. Factor H and factor I are soluble complement-activation inhibitors, and preincubation of factor I with Aβ in the presence of factor H abolished the ability of Aβ to cleave C3b, and also abolished the ability of factor I to cleave FGR-AMC. In contrast, Aβ did not affect the function of factor H even after binding. The production of iC3b was significantly decreased when C3b and factor H were incubated with the eyes from neprilysin gene-disrupted mice as compared with when C3b and factor H were incubated with eyes from age-matched wild-type mice. These results suggest that Aβ activates the complement system within drusen by blocking the function of factor I leading to a low-grade, chronic inflammation in subretinal tissues. These findings link four factors that have been suggested to be associated with AMD: inflammation, complement activation, Aβ deposition, and drusen. *The Journal of Immunology,* **2008, 181: 712–720.**

The complement system is a component of the humoral immune system involved in host defense, and it can be activated through three distinct pathways: the classical, the alternative, and the lectin. Activation of these three pathways leads to the cleavage of C3 into C3a and C3b (1), which finally leads to the formation of the C5b-9 membrane attack complex (MAC)[3] (1–3). The MAC is a lytic complex that is lethal not only to foreign pathogens but also to local host cells and tissues. Thus, the regulation of complement activation is important for the maintenance of tissue homeostasis and is mediated by a family of complement proteins.

There has recently been an increased interest in the involvement of complement in the development and progression of many diseases including age-related macular degeneration (AMD). AMD is the leading cause of irreversible vision loss, affecting 30~50 million elderly individuals worldwide (4–7). Two major clinical phenotypes of AMD are recognized: a nonexudative (dry) type and an exudative (wet) type. Recent studies have demonstrated that local and chronic inflammation induced by the complement pathway plays a central role in the formation of drusen and the development of AMD (8–11).

Polymorphisms in the genes coding for complement factor H and factor B have been shown to be predictors of the risk of developing AMD (12–17). Factor H and factor B are key components of the alternative complement pathway. Factor H, the most important soluble complement activation inhibitor, blocks the binding of factor B to C3b, supports the dissociation of the C3bBb complex (decay-accelerating activity), and acts as a cofactor in the cleavage of C3b by factor I (18, 19). Another susceptible locus for AMD is the hypothetical gene called *LOC387715/HTRA1* (17, 20–22). The population risk associated with variants of factor H, factor B, and *LOC387715/HTRA1* is at least 50% (17). In addition, a very recent study confirmed that functional polymorphisms in the *C3* gene were strongly associated with AMD (23). These genetic studies in patients with AMD, together with the finding that proteins associated with inflammation and immune-mediated processes are deposited in drusen and Bruch's membrane in eyes with AMD (24), support the hypothesis that inflammation and complement activation are involved in the pathogenesis of AMD. Also, animal experiments, using a laser-induced choroidal neovascularization model, showed that the activation of the complement alternative

*Department of Ophthalmology and Visual Science, Tokyo Medical and Dental University, Tokyo, Japan; †Section of Cellular Physiological Chemistry, Tokyo Medical and Dental University, Tokyo, Japan; and ‡Laboratory for Proteolytic Neuroscience, Institute of Physical and Chemical Research (RIKEN) Brain Science Institute, Wako-shi, Saitama, Japan

Received for publication November 13, 2007. Accepted for publication April 29, 2008.

The costs of publication of this article were defrayed in part by the payment of page charges. This article must therefore be hereby marked *advertisement* in accordance with 18 U.S.C. Section 1734 solely to indicate this fact.

[1] This work was supported in part by Research Grants 19390441, 18023037, and 19659445 from the Japan Society for the Promotion of Science, Tokyo, Japan. This work was supported in part by Grants-in-Aid for Scientific Research on Priority Areas, Research on Pathomechanisms of Brain Disorders 18023037 (to N.I.) and 20023031 (to N.I.) from the Ministry of Education, Culture, Sports, Science, and Technology, Japan.

[2] Address correspondence and reprint requests to Dr. Kyoko Ohno-Matsui, Department of Ophthalmology and Visual Science, Tokyo Medical and Dental University, 1-5-45 Yushima, Bunkyo-ku, Tokyo 113, Japan. E-mail address: k.ohno.oph@tmd.ac.jp

[3] Abbreviations used in this paper: MAC, membrane attack complex; AMD, age-related macular degeneration; RPE, retinal pigmented epithelium; Aβ, amyloid β; AD, Alzheimer's disease; FGF, fibroblast growth factor; FHL, factor H-like protein.

pathway was critical for the development of choroidal neovascularization (25), a major feature of the neovascular form of AMD.

One of the earliest clinical hallmarks of AMD is subretinal extracellular deposits, known as drusen, which accumulate beneath the retinal pigmented epithelium (RPE) (26). Epidemiological studies have shown that numerous and/or confluent drusen significantly increase the risk for the development of AMD (27, 28). However, the mechanism of the development of AMD from drusen has not been precisely determined. Recent proteomic analyses have shown that drusen contain many proteins, such as cholesterol, apolipoproteins B and E, C-reactive protein, clusterin, vitronectin, and amyloid β (Aβ) (24, 29, 30). Among these proteins, we focused on Aβ as the primary stimulus that causes the development of AMD (31).

Aβ peptides vary in length from 39- to 43-aa residues and are produced by the sequential proteolytic processing of amyloid precursor proteins. Studies have shown that Aβ is the main component of senile plaques in the brain of patients with Alzheimer's disease (AD), and the transition of Aβ from the monomeric form to the oligomeric or aggregated form in the brain is a key event in the pathogenesis of AD (32–34). The results of our earlier study demonstrated that exposure of RPE cells to Aβ induced a marked increase in vascular endothelial growth factor and a marked decrease of pigment epithelium-derived factor, an antiangiogenic factor, in the RPE cells (31). Importantly, there was an increase in the deposition of Aβ in the subretinal space of senescent neprilysin gene-disrupted mice, and these mice developed several features of human eyes with AMD (31). These results suggest that Aβ deposited in drusen may be a key contributor to the development of AMD. However, the underlying molecular mechanism on how Aβ leads to the features of AMD has not been determined.

The pathogenesis of AD has also been considered to be one of the inflammatory processes caused by complement activation (35). Aβ is colocalized with activated complement components, the C5b-9 MAC, in the brain of AD patients (36). Aβ activates the alternative pathway by triggering the formation of covalent, ester-linked complexes of Aβ with C3b/iC3b, an activation product of the third complement component (C3) (36). Also in AMD, Johnson et al. (29) demonstrated that Aβ is colocalized with the activation-specific fragments of complement C3 in unique substructural domains, the "amyloid vesicles," within the drusen thereby identifying them as potential sites of complement activation.

These findings led us to hypothesize that AMD results from an abnormal inflammatory process which includes an unregulated activation of the complement pathway triggered by Aβ, as suggested for AD. Although there has been a publication demonstrating the colocalization of complement proteins and Aβ in eyes with AMD (29), the precise mechanism of how complement is activated by Aβ in AMD has not been determined. Based on the human pathological studies and our previous animal experiments, we have explored the influence of Aβ on the activation of the alternative pathway, and we will present new evidence that Aβ binds and inactivates the function of complement factor I. This then results in an unregulated activation of complement in subretinal tissues.

Materials and Methods

Materials

DMEM, TRIzol reagent, and the SilverQuest silver staining kit were purchased from Invitrogen; plastic ware (Falcon) was obtained from BD Biosciences; FCS was obtained from HyClone; human recombinant basic fibroblast growth factor (FGF) was obtained from R&D Systems; laminin was obtained from Upstate Biotechnology; You-Prime First-Strand Beads, PCR beads, and nylon membranes were obtained from Amersham Pharmacia Biotech; agarose was obtained from Takara; $A\beta_{1-40}$ (HCl form) and $A\beta_{40-1}$ were obtained from Peptide Institute. The mAb against Aβ (4G8) was purchased from SIGNET; the iC3b ELISA kit, purified human factor H, and purified human factor I were obtained from Quidel; purified human C3b was obtained from Biogenesis; mAb against human factor I (MCA507, OX21), mAb against human factor H (MCA509, OX24), and polyclonal antiserum against human C3 (AHC007) were obtained from Serotec; recombinant substrate FGR-AMC was obtained from American Diagnostica; Microfluor white plates were obtained from Packard Bioscience; the0.4-μm pore-size transwell was obtained from Corning; the XTT cell proliferation assay kit was obtained from Cayman Chemical.

Human RPE cell cultures

Primary cultures of human RPE cells were a gift from Dr. P. A. Campochiaro (Wilmer Eye Institute, Johns Hopkins University, Baltimore, MD). The cultures used for the experiments were at the third or fourth passage at the time of separation. Cultures were shown to be pure populations of RPE cells by immunocytochemical staining for cytokeratins (data not shown). Differentiated RPE cells were established as described (37, 38). RPE cell cultures were maintained in DMEM supplemented with 10% FBS and 10 ng/ml basic FGF. The cells exhibited epithelial morphology and expressed CRALBP, a marker for differentiated RPE cells (38).

RPE cells were subcultured in 12-well tissue-culture plates at a density of 6×10^4 cells/well. Seven days after reaching confluence, the medium was changed, and cells were incubated in serum-free DMEM (500 μl) in the presence (50 μM) or absence of $A\beta_{1-40}$ peptide (HCl form). After 24 h, the medium was collected and stored at −20°C until use for Western blot analysis and ELISA. The cells were homogenized, and their RNA and protein were extracted. Each condition was examined in triplicate, and results were repeated in at least three independent experiments.

Cell viability assay

Seven days after reaching cellular confluence, the medium was changed, and cells were incubated in serum-free DMEM in the presence (25 or 50 μM) or absence of $A\beta_{1-40}$ peptide (HCl form) for 24 h. The XTT assay was used to measure viability using XTT reagent (Cayman Chemical), which was added for 1 h at 37°C and was quantified using an ELISA plate reader. The average absorbance measured for medium plus treatment was subtracted from each test sample. Each experiment was performed at least three times on different days.

RT-PCR for C3, C5, factor H, factor H-like protein (FHL), factor B, and factor I

Total RNA was extracted from cultured RPE cells using TRIzol reagent. cDNA was synthesized from 2 μg of total RNA using You-Prime First-Strand Beads according to the manufacturer's protocol, and the reaction products were subjected to PCR amplification using the GeneAmp PCR system (Cetus; PerkinElmer). The mRNAs of human C3, C5, factor H, FHL (a truncated form of factor H (39)), factor B, and factor I were amplified with the following primers: for C3 (40), 5′-TCACCGTCAACC ACAAGCTGCTACC-3′ (forward) and 5′-TTTCATAGTAGGCTCGGA TCTTCCA-3′ (reverse); for C5 (40), 5′-GTGGCATTAGCAGCAGTG GACAGTG-3′ (forward) and 5′-GCAGGCTCCATCGTAACAACATT TC-3′ (reverse); for factor H (41), 5′-TCTGCATGTTGGCCTTCCT GTC-3′ (forward) and 5′-CTTCCTTGTAAATCTCCACCTG-3′ (reverse); for FHL (40), 5′-CAGAAGTTCAGAGGGTAAAGCT-3′ (forward) and 5′-TACTGGCTGGATACCTGCTCCG-3′ (reverse); for factor B (42), 5′-CAACAGAAGCGGAAGATCGTC-3′ (forward) and 5′-TAT CTCCAGGTCCCGCTTCTC-3′ (reverse); and for factor I (43), 5′-GGC AGGTGGCAATTAAGGATG-3′ (forward) and 5′-GGTGTATCCAGT CTACTACTGT-3′ (reverse).

The PCR for factor H and FHL was repeated for 30 cycles, and each cycle included denaturation at 94°C for 1 min, annealing at 58°C for 1 min, and primer extension at 72°C for 1 min. The PCR for C3 and C5 was repeated for 30 cycles, and each cycle included denaturation at 94°C for 1 min, annealing at 62°C for 1 min, and primer extension at 72°C for 1 min. The PCR for factor I was repeated for 30 cycles, and each cycle included denaturation at 94°C for 1 min, annealing at 60°C for 1 min, and primer extension at 72°C for 1 min. The PCR for factor B was repeated for 35 cycles, and each cycle included denaturation at 94°C for 1 min, annealing at 59°C for 1 min, and primer extension at 72°C for 1 min. The expected size of the reaction products was 186 bp for C3, 315 bp for C5, 424 bp for FHL, 354 bp for factor H, 884 bp for factor B, and 146 bp for factor I.

LightCycler real-time PCR

The cDNA was subjected to quantitative PCRs on a LightCycler Instrument (Roche Diagnostics) using the QuantiTect SYBR Green PCR kit (Qiagen) for C3, factor H, and factor I. PCR amplifications were performed

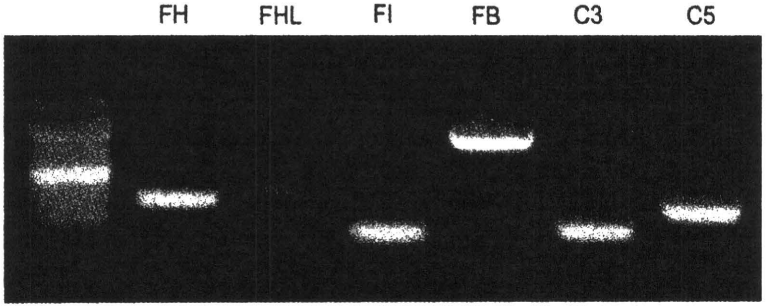

FIGURE 1. RT-PCR detection of complement proteins and their regulators in cultured human RPE cells. Human RPE cells were cultured in DMEM containing 10% FCS and 10 ng/ml basic FGF. After attaining confluence, total RNA was extracted from cultured RPE cells. cDNAs were synthesized from 2 μg of total RNA, and the reaction products were subjected to PCR amplification using specific primers for each factor. FH, Factor H; FI, factor I; FB, factor B.

with specific primers in a total volume of 20 μl containing 2 μl of sense and antisense primer mixture (0.5 μM of each primer), 10 μl of 2× SYBR Green QPCR Master Mix (Qiagen), 1 μl of 1/10 diluted cDNA, and 7 μl of nuclease-free PCR-grade water. The mixture was used as a template for the amplification after initial denaturation at 95°C and 40~50 cycles (95°C for 10 s, 58~62°C for 15 s, and 72°C for 30 s). The primer sequences of human GAPDH were 5′-ACCACAGTCCATGCCATCAC-3′ (forward) and 5′-TCCACCACCCTGTTGCTGTA-3′ (reverse). The primer sequences of C3, factor H, factor B, and factor I were the same as used for semiquantitative RT-PCR. SYBR Green fluorescence was measured, and quantification of each PCR product was expressed relative to GAPDH.

ELISA measurements of C3 fragments

The amount of iC3b secreted from RPE cells into the conditioned medium was determined with a commercial ELISA kit according to the manufacturer's instructions. The absorbance was measured at 405 nm in a Bio-Rad Model 450 microplate reader. Serial dilutions of recombinant C3 and iC3b were measured and a standardized curve was constructed.

Five days after cellular confluence, the medium was changed to serum-free DMEM. Then, the cells were incubated with or without $A\beta_{1-40}$ (HCl form; 50 μM) or $A\beta_{40-1}$ for 24 h. In some experiments, exogenous C3b (5 μg/ml) was added to the medium, and in other experiments, cells were preincubated with or without $A\beta_{1-40}$ (HCl form; 50 μM) for 12 h. After the preincubation, C3b (5 μg/ml) and various concentrations of purified human factor H or factor I were added to the medium. The conditioned media were collected after another 12 h, and the amount of iC3b was measured.

For transwell membrane experiments, cultured RPE cells were seeded onto cell culture inserts (0.4-μm pore size; Costar; Corning). Five days after cellular confluence, the medium was changed to serum-free DMEM. In this experiment, the exogenous C3b and $A\beta_{1-40}$ were added into the lower chamber. The conditioned media were also collected from the lower chamber.

Because it has already been reported that mouse complement factor I can cleave human C3b in the presence of human complement factor H (44), the ability of cleaving human C3b by the eye samples from both 12-mo-old neprilysin gene-disrupted mice (which leads to an increased deposition of Aβ as we demonstrated previously (31)) and age-matched wild-type mice was examined. Briefly, eyes were enucleated and the anterior segment as well as the neural retina was removed from the eyecup before sclera and the vascular choroid were carefully removed as much as possible using forceps. Electron microscopic examination confirmed that the intact RPE-Bruch's membrane-choriocapillaris complex and only a small amount of vascular choroid were removed in preliminary experiments (data not shown). The RPE-Bruch's membrane-choriocapillaris complex was pooled from four eyes, respectively, from wild-type or neprilysin gene-disrupted mice, and then were transferred into 1.5-ml assay tubes containing 40 μl of 10 μM phosphate buffer (pH 7.4; containing 145 mM NaCl) including 3.2 μg of human C3b and 3.2 μg of human factor H. The mixtures were centrifuged and incubated at 37°C for 12 h before being submitted to human iC3b EIA.

Western blot analyses

For the Western blot analysis of C3, factor H, and factor I, RPE cells were maintained in serum-free medium for 24 h; the conditioned media were collected and cells were lysed in 1 ml of sample buffer (125 mM Tris-HCl (pH 6.8), 2% SDS, 5% glycerol, 0.003% bromphenol blue, and 1% 2-ME). The final protein concentration was determined using a BCA assay (Pierce) according to the manufacturer's instructions. Equal amounts of secreted protein (8 μg) or a sample of the whole cell lysate (80 μg) were separated by 8% SDS-PAGE and electrophoretically transferred onto nylon membranes. The nylon membranes containing the transferred proteins were pretreated with 5.0% nonfat dried milk in 50 mM Tris (pH 8.0) and then incubated overnight with a monoclonal Ab against human C3 (1/1000 dilution), mAb against human factor H (1/200 dilution), or mAb against human factor I (1/200 dilution). SDS-PAGE analysis for C3, factor H, and factor I was performed under nonreduced conditions.

Measurement of factor I cofactor activity

The cleavage of C3b by factor I in the presence of factor H was performed in 10 mM phosphate buffer (pH 7.4) containing 145 mM NaCl, according to the method of Sahu et al. (45) In a typical assay, C3b (80 ng/μl), factor H (80 ng/μl), and factor I (3.5 ng/μl) were mixed in 10 μM phosphate buffer (pH 7.4; containing 145 mM NaCl). The total volume in each reaction tube was adjusted to 20 μl, and the tube was incubated at 37°C. In some experiments, factor I and/or factor H were preincubated with $A\beta_{1-40}$ (200 μM) for 1 h, and then incubated with C3b. After another 1 h, samples (5 μl) were removed and mixed with sample buffer containing DTT, boiled for 5 min, and subjected to electrophoresis on an 8% SDS-PAGE gel. The cleavage products were made visible by silver staining of the gel.

Amidolytic assay using synthetic substrate

The cleavage of the synthetic FGR-AMC by factor I in the presence or absence of Aβ was examined. This substrate is cleaved by factor I in the absence of any cofactors (46). FGR-AMC (50 μM; final concentration) in 20 mM HEPES at pH 8.5 was added to factor I (0.5 μM; final concentration) in the same buffer in a white Microfluor plate. The final reaction volume was 200 μl. The reaction was performed in the presence or absence of $A\beta_{1-40}$ (200 μM, final concentration). The amidolytic activity of factor I was measured using a microtiter plate reader (Fluoroskan; Thermo Life Sciences) by excitation at 355 nm and continuous monitoring of emission at 460 nm for 1 h or more at 37°C. Activity of factor I was expressed as fluorescence of total free AMC released from FGR-AMC by the cleavage of factor I.

Coimmunoprecipitation

To examine the binding of factor I or factor H and Aβ, human purified factor I (210 ng) or human purified factor H (4.8 μg) and $A\beta_{1-40}$ (200 μM; final concentration) were added to 10 μM phosphate buffer (pH 7.4; containing 145 mM NaCl) to a final volume of 60 μl. After 1-h incubation at 37°C, the mixtures were reacted with 200 μl of factor I Ab or 200 μl of factor H Ab and further incubated at 4°C with gentle end-over-end mixing for 90 min. After incubation, 100 μl of 50% agarose slurry (protein G type) was added to both mixtures and further incubated at 4°C for 30 min with gentle end-over-end mixing. After 30 min of incubation, each mixture was centrifuged, the supernatant was removed, and the agarose containing factor I-Aβ complex or factor H-Aβ complex was washed with PBS three times before being loaded in diluted sample buffer (by PBS, 1/1) which did not contain DTT. The samples was heated for 5 min at 100°C and centrifuged. Then, 50 μl of the supernatant from each sample was respectively subjected to Western blot analysis using factor I Ab (MCA507, 1/200) or factor H Ab (MCA509, 1/200), and Aβ (4G8, 1/1000) Ab. Complex immunoreactivity was made visible by exposure of x-ray film to blots incubated with ECL reagent.

Statistical analyses

Data are expressed as means ± SEM. The significance level was set at $p < 0.05$. Statistical analysis was performed with the Mann-Whitney U test.

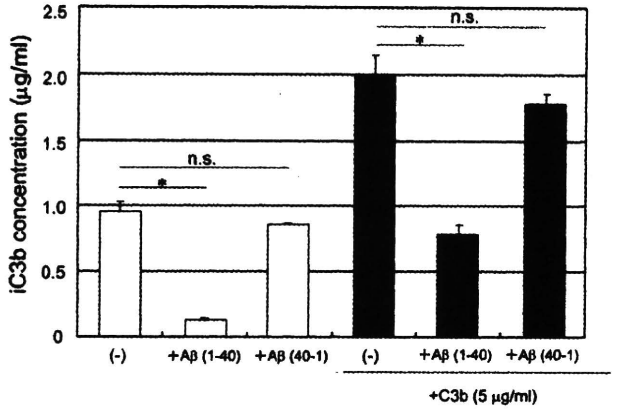

FIGURE 2. Concentration of immunoreactive iC3b in the supernatant of cultured RPE cells. Human RPE cells were incubated in the presence (50 μM) or absence of Aβ and/or C3b (5 μg/ml). The expression of iC3b protein in the culture supernatants was analyzed by ELISA after 24 h of culture. Values are expressed as the means ± SEMs. $n = 4$, *, $p < 0.05$.

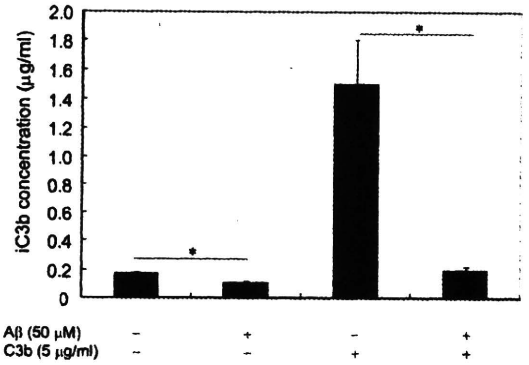

FIGURE 3. Decreased production of iC3b in the RPE cells in the presence of $A\beta_{1-40}$ using the transwell culture system. Cultured RPE cells were seeded into Costar cell culture inserts (0.4-μm pore size; Corning). Five days after cellular confluence, the medium was changed to serum-free DMEM. In this experiment, the exogenous C3b and $A\beta_{1-40}$ were added into the lower chamber. The conditioned media were also collected from the lower chamber, and the amount of iC3b was measured using ELISA, $n = 3$. *, $p < 0.05$.

Results

Expression of C3, C5, factor H, FHL, factor B, and factor I in RPE cells

The liver is the primary site of synthesis of the majority of the complement proteins in the human plasma. Extrahepatic biosynthesis of complement proteins may be an important factor in triggering and perpetuating local inflammatory reactions, especially in tissues that are shielded from the plasma components by a blood-tissue barrier. RT-PCR demonstrated the constitutive expression of the mRNAs for C3, C5, factor H, FHL, factor B, and factor I (Fig. 1) in the RPE cells. These findings suggest that RPE cells have a capacity to modulate the activation of the alternative pathway of complement.

C3b degradation is inhibited in Aβ-treated RPE cells

In all three pathways of complement activation, the pivotal step is the conversion of complement C3 to C3b, which is then covertly coupled to pathogens and Ag-Ab complexes. C3b is cleaved by factor I to iC3b in the presence of factor H and other cofactors (47). To determine whether C3b was cleaved by the RPE cells, we measured the level of iC3b in the supernatant by ELISA. Without exogenous C3b and $A\beta_{1-40}$, the average level of iC3b was 0.95 ± 0.08 μg/ml in the supernatants of RPE cells (Fig. 2). When the RPE cells were incubated with 50 μM $A\beta_{1-40}$ for 24 h, the amount of iC3b was significantly reduced to 0.13 ± 0.01 μg/ml ($p = 0.007$). When C3b (5 μg/ml) was added to the medium, the average amount of iC3b in the RPE cell supernatant was significantly increased to 2.00 ± 0.14 μg/ml. However, when 50 μM $A\beta_{1-40}$ was added to the medium, the amount of iC3b was significantly decreased to 0.78 ± 0.07 μg/ml ($p = 0.013$). In contrast, $A\beta_{40-1}$ alone had no effect on the cleavage of C3b.

When we added the $A\beta_{1-40}$ into the lower chamber using the transwell culture system, the amount of iC3b within the medium from the lower chamber was significantly decreased to 0.11 ± 0.01 μg/ml as compared with 0.175 ± 0.005 μg/ml within the medium from the nontreated RPE cells ($p = 0.034$) (Fig. 3). When C3b (5 μg/ml) was added into the lower medium, the average amount of iC3b was significantly increased to 1.5 ± 0.3 μg/ml. However, when 50 μM $A\beta_{1-40}$ was added to the lower medium together with C3b, the amount of iC3b was significantly decreased to 0.2 ± 0.02 μg/ml ($p = 0.0016$) (Fig. 3). In addition, the 50 μM $A\beta_{1-40}$ did not affect the cell viability as determined by the XTT assay (data not shown).

Addition of factor I restores iC3b production in Aβ-treated RPE cells

To confirm the direct contribution of either factor I or factor H in the decrease of C3b degradation by Aβ, we then examined the effect of purified factor I or factor H on Aβ-induced degradation of C3b. After changing the medium to serum-free medium, RPE cells were preincubated with (50 μM) or without $A\beta_{1-40}$ for 12 h. Then, 5 μg of rC3b was added to the medium, and the supernatant was collected after another 12 h. The amount of iC3b was determined by ELISA. The concentration of iC3b in the supernatants of nontreated RPE cells was 2.30 ± 0.10 μg/ml (Fig. 4), but the iC3b was significantly decreased to 0.87 ± 0.05 μg/ml in Aβ-treated RPE cells ($p = 0.013$). The addition of human purified factor I (1, 2, and 5 μg) significantly restored iC3b generation, but the addition of purified factor H (1, 2, and 5 μg) did not increase the amount of

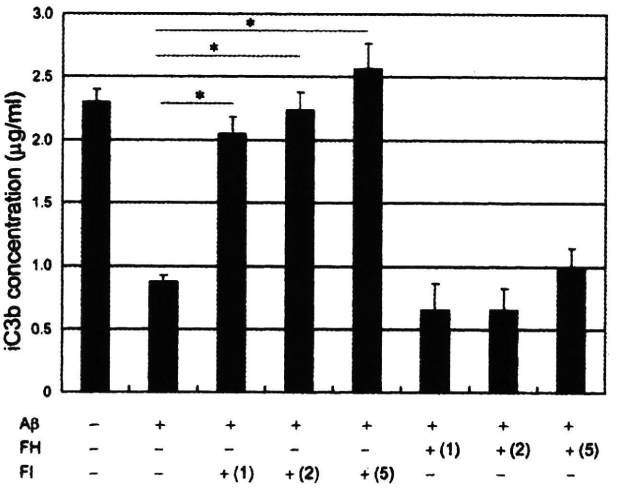

FIGURE 4. Effects of the addition of purified factor I or factor H on iC3b production in human RPE cells treated or not treated with Aβ. Twelve hours after changing the medium to serum-free DMEM supplemented with 50 μM Aβ and 5 μg/ml rC3b, purified factor H or factor I in different concentrations (1, 2, and 5 μg/ml) were added. After incubation for 12 more hours, the supernatants were collected and analyzed by ELISA for iC3b, $n = 3$. *, $p < 0.05$; FH, factor H; FI, factor I.

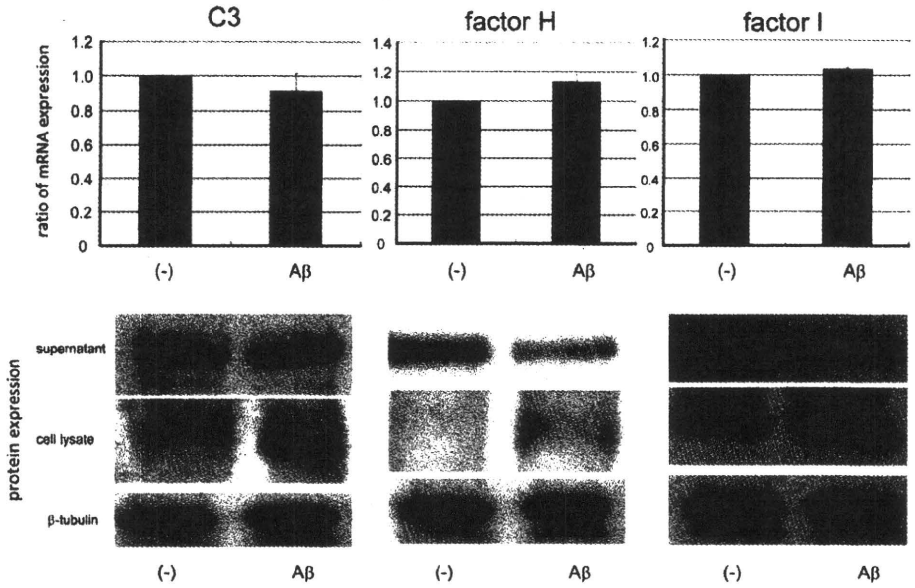

FIGURE 5. *Upper lane*, Real-time PCR analysis of cDNA of C3 (*left*), factor H (*center*), and factor I (*right*) prepared from RNA isolated from cultured human RPE cells in the presence or absence of Aβ (50 μM) for 24 h. The levels of mRNA are standardized to the level of GAPDH. The levels of mRNA of Aβ-treated RPE cells are shown as a ratio of those of nontreated RPE cells, and the averages of three samples (±SEMs) are plotted. Data are from five independent experiments. *Lower lane*, Immunoblot of C3 (*left*), factor H (*center*), and factor I (*right*) in cell lysates and the supernatants from human RPE cells in the presence or absence of 50 μM Aβ for 24 h. The supernatants (20 μl/lane) or cell lysates (80 μg/lane) were separated by SDS-PAGE, blotted onto nylon membrane, and detected with polyclonal anti-C3 (*left*), anti-factor H (*center*), or anti-factor I (*right*). This is a representative figure of five independent experiments.

iC3b, although the high concentration of factor H (5 μg) was able to restore iC3b generation in part.

Effects of Aβ on expression of gene and protein of C3, factor H, and factor I in human RPE cells

To determine whether the decrease of iC3b in the Aβ-treated RPE cells was due to a modified production of different complement-related proteins, we determined the expression of the mRNA and protein of C3, factor H, and factor I. The results showed that the expressions of the mRNA of C3, factor H, and factor I were not significantly different between RPE cells with and without Aβ treatment by real-time PCR ($p > 0.05$; Fig. 5, *upper lane*).

A representative photograph of a Western blot of C3, factor H, and factor I protein is shown in Fig. 5. Compared with nontreated RPE cells, the amount of C3 protein in the supernatants of Aβ-treated cells was similar, although it was slightly higher than that in the cell lysates. The secretion of factor H protein was decreased more in the supernatant of RPE cells treated with $Aβ_{1-40}$ than that in nontreated cells, and factor H protein was also increased in the Aβ-treated RPE cell lysates compared with nontreated cell lysates. The secretion of the protein of factor I was decreased more in the supernatant of Aβ-treated RPE cells than in nontreated cells; however, factor I protein was slightly increased in the cell lysates of Aβ-treated cells than in nontreated cell lysates.

Binding of Aβ with factor H and factor I

Because it has already been reported that Aβ binds to factor H (48), we investigated whether Aβ also forms a complex with factor I. Coimmunoprecipitation analysis detected a band in the 88-kDa area, which corresponded to the molecular mass of factor I, both

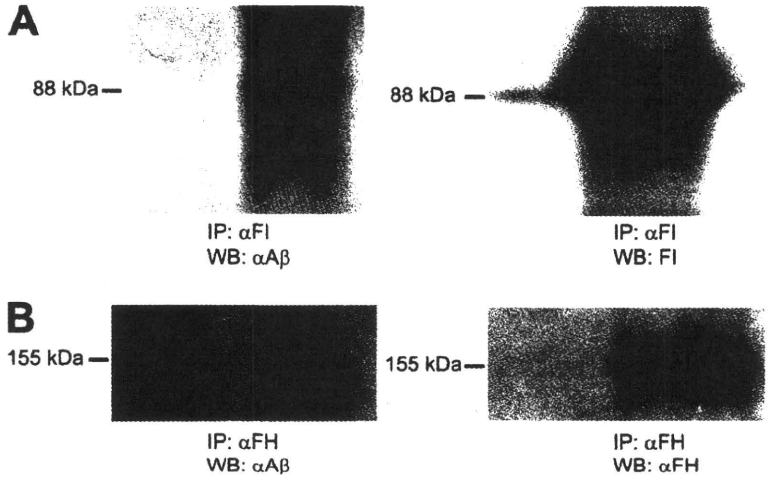

FIGURE 6. Coimmunoprecipitation of factor I-Aβ complex (*A*) and factor H-Aβ complex (*B*). Aβ and factor I or factor H were incubated in phosphate buffer (pH 7.4) for 1 h at 37°C before being loaded with factor I Ab or factor H Ab and further incubated at 4°C with gentle end-over-end mixing. Then, 50% agarose slurry (protein G type) was added to the mixture and further incubated at 4°C. Total mixture was centrifuged, supernatant was removed, and agarose-containing factor I-Aβ complex or factor H-Aβ complex was washed in PBS. The sample was centrifuged and the supernatant was subjected to Western blot analysis. The band in the 88-kDa area corresponding to factor I was detected by both factor I Ab (MCA507, 1/200) and Aβ Ab (4G8, 1/1000) (Fig. 5*A*). The band in the 155-kDa area corresponding to factor H was detected by both factor H Ab (MCA509, 1/200) and Aβ Ab (4G8, 1/1000) (Fig. 5*B*). FH, Factor H; FI, factor I; IP, immunoprecipitation; WB, Western blotting.

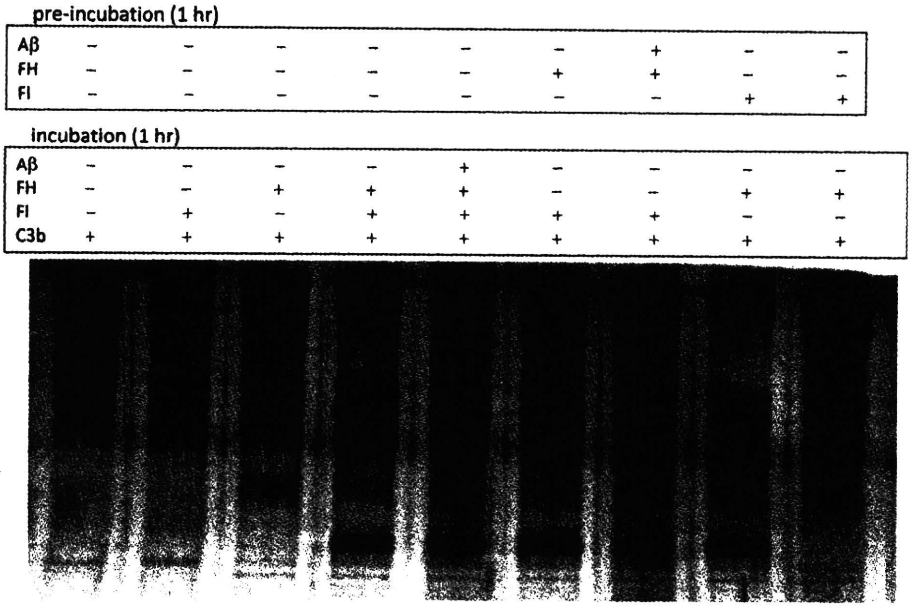

FIGURE 7. Preincubation of factor I with Aβ inhibits the cleavage of α-chain of C3b in a cofactor assay. Factor H and/or factor I were preincubated or not preincubated with Aβ (200 μM) for 1 h, and then mixed with C3b for another 1 h. All of the reactions were performed at 37°C in 10 μM phosphate buffer (pH 7.4) containing 145 mM NaCl and the reaction was stopped by the addition of SDS-PAGE buffer containing 2-ME. The reaction mixture was loaded onto 8% SDS-PAGE gel, and the cleavage products were made visible by silver staining. This is a representative photograph of five independent experiments. FH, Factor H; FI, factor I.

by Abs against factor I as well as against Aβ (Fig. 6*A*). Also, a band in the 155-kDa area, which corresponded to the molecular mass of factor H, was detected by the Abs against factor H and Aβ (Fig. 6*B*). These findings indicated that Aβ binds to factor I as well as factor H to form a complex.

Aβ affects activity of factor I but not factor H

We next analyzed whether Aβ affected the ability of factor I and factor H to cleave C3b. When C3b was incubated in only phosphate buffer, we detected two bands corresponding to the α- (110-kDa) and β- (70-kDa) chains of C3b (Fig. 7, *first lane*). The addition of factor H or factor I alone did not cause the degradation of C3b (Fig. 7, *second* and *third lanes*). When we incubated C3b with both factor H and factor I, two degradative fragments of the α-chain, viz., 68- and 43-kDa, appeared (Fig. 7, *fourth lane*). The absence of the 68- and 43-kDa fragments in reactions with C3b and factor I or factor H alone showed that both factor I and factor H are necessary for the cleavage of C3b under these conditions (Fig. 7, *fourth lane*). The presence of the 68- and 43-kDa fragments indicated that factor I mediated the cleavage of C3b between Arg^{1298} and Ser^{1299} in the generation of $iC3b_2$. Finally, when we simultaneously incubated C3b with factor H, factor I, and $A\beta_{1-40}$, the α-chain of C3b was also cleaved into two fragments (Fig. 7, *fifth lane*).

Next, we investigated whether preincubation of factor H or factor I with Aβ affected its ability to cleave of C3b. When factor H

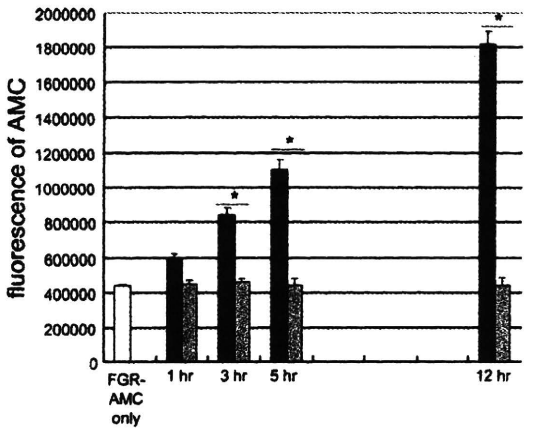

FIGURE 8. Amidolytic assay using synthetic substrate FGR-AMC. FGR-AMC (50 μM) and factor I (0.5 μM) in the presence (▨) or the absence (■) of 200 μM Aβ were incubated in 20 mM HEPES (pH 8.5) and at 37°C under light protection. Fluorescence of released AMC was measured by the excitation at 355 nm and emission at 460 nm, at different time points, $n = 3$; *, $p < 0.05$.

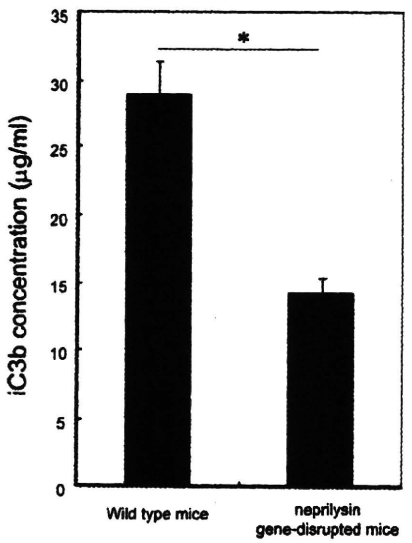

FIGURE 9. Decreased production of iC3b when C3b and factor H were incubated with the RPE-Bruch's membrane complex of neprilysin gene-disrupted mice as compared with that when C3b and factor H were incubated with the RPE-Bruch's membrane complex of wild-type mice. The RPE-Bruch's membrane-choriocapillaris complex was extracted from each four eyes of wild-type mice and neprilysin gene-disrupted mice. These complexes were then transferred into 40 μl of 10 μM phosphate buffer (pH 7.4; containing 145 mM NaCl) with C3b and factor H and incubated at 37°C for 12 h. After incubation, the supernatants were collected, diluted by 25 times in 10 μM phosphate buffer (pH 7.4, containing 145 mM NaCl), before being submitted to ELISA for iC3b. FH, Factor H; $n = 3$; *, $p < 0.05$.

was preincubated with $A\beta_{1-40}$ for 1 h, and then incubated with C3b and factor I for an additional 1 h, the degradation of the α-chain occurred (Fig. 7, *seventh lane*). However, when factor I was preincubated with $A\beta_{1-40}$ for 1 h before with C3b and factor H for another hour, the degradation of α-chain did not occur (Fig. 7, *ninth lane*). These results indicated that the preincubation with Aβ affected the ability of factor I, but not factor H, to cleave C3b into iC3b.

Effects of Aβ on the amidolytic activity of factor I

To further explore whether Aβ affected the function of factor I, we examined the amidolytic activity of factor I. This assay determines the levels of amidolytic activity of factor I against the FGR-AMC substrate without any cofactors. The addition of $A\beta_{1-40}$ abolished the amidolytic activity of factor I for 1–12 h (Fig. 8).

C3b degradative activity is decreased in the eyes of neprilysin gene-disrupted mice

Finally, we incubated the RPE-Bruch's membrane-choriocapillaris complex from the eyes of 12-mo-old neprilysin gene-disrupted mice or age-matched wild-type mice with exogenously added human C3b and factor H. The results demonstrated that the production of iC3b was significantly decreased to 14.2 ± 1.25 μg/ml when C3b and factor H were incubated with the eyes from neprilysin gene-disrupted mice compared with when C3b and factor H were incubated with the eyes from wild-type mice (29.0 ± 2.5 μg/ml; $p = 0.049$; Fig. 9).

Discussion

In our previous study regarding the developmental mechanism of AMD from drusen, (31) we focused on Aβ accumulated within drusen, and demonstrated that senescent neprilysin gene-disrupted mice which accumulate an excess amount of Aβ manifested similar features of human AMD. Although the mechanism for why Aβ induced the development of AMD was unclear, we hypothesized that Aβ-induced complement activation in subretinal tissue plays an important role for the development of AMD, and explored the mechanism of Aβ-induced complement activation in the present study.

Our results showed that the generation of inactivated C3b, and thus iC3b, was inhibited in RPE cells exposed to Aβ (Fig. 2). This finding was confirmed in experiments using the RPE-Bruch's membrane-choriocapillaris complex from neprilysin gene-disrupted mice (Fig. 9), which accumulated Aβ deposition in RPE cells as well as within the sub-RPE deposits, as we reported previously (31). The mechanism for this inhibition is the binding of Aβ to factor I which abolishes its ability to cleave its substrates as shown in two functional assays: the cofactor assay and the amidolytic assay.

Factor I is an 88-kDa serum glycoprotein which is a serine protease and cleaves the α-chains of C3b and C4b in the presence of its cofactor proteins (46). By inactivating C3b and C4b through limited proteolytic cleavage and thereby preventing the formation of the C3 and C5 convertases, factor I inhibits the alternative and the classical component pathways. Thus, the dysfunction of factor I accelerates the formation of the C3 convertase in the alternative pathway (45) resulting in unregulated complement activation.

Interestingly, the simultaneous incubation of Aβ with C3b, factor H, and factor I did not inhibit the C3b degradation in the cofactor assay. However, preincubation of factor I with Aβ abolished its ability to cleave the α-chain of C3b in the cofactor assay and to cleave FGR-AMC in the amidolytic assay. The HCl form of Aβ is known to be aggregated within 30 min when incubated in medium by The Peptide Institute (Osaka, Japan). This might suggest that the aggregation of Aβ might be necessary for the binding to factor I to Aβ as shown for the binding of factor H to Aβ (48). However, the mechanism of how the function of factor I is disturbed after binding to Aβ requires further investigation. As best we know, the binding of factor I to Aβ has not been reported, while the binding of factor H to the aggregated fibrillar form of Aβ has been reported (48). Aggregated fibrillar Aβ is generally considered to be a rather sticky complex capable of binding proteins nonspecifically, although a charge-based interaction might be one possibility as suggested by Strohmeyer and associates (48).

Western blot analyses showed that exposure of RPE cells to Aβ decreased the amount of factor H and factor I secreted into the supernatant of cultured RPE cells (Fig. 5), while Western blot analyses using cell lysates showed that the amount of C3, factor H, and factor I was increased in Aβ-treated RPE cells (Fig. 5). This difference might be because Aβ binds to these molecules and traps them possibly on the cell membrane as reported (43). Thus, not only the dysfunction of factor I by binding to Aβ, but also a decrease of the secreted amount of free factor H and factor I into the subretinal space might be involved in the process of the unregulated activation of complement.

The extrahepatic biosynthesis of complement is considered to be an important source of complement which triggers and perpetuates local inflammatory reactions, especially in tissues that are shielded from the plasma components by a blood-tissue barrier such as the retina. By using specific primers and RT-PCR, we demonstrated that human RPE cells constitutively express the major components of the complement alternative pathway, including C3, factor B, factor H, FHL, C5, and factor I (Figs. 1 and 2). A Medline search identified only one publication that reported the synthesis of factor H by human and mouse RPE cells (49). However, we did not find any publications for the expression of the other complement components by RPE cells.

The expression of various complement components in human RPE cells suggests that most of the complement proteins and their regulators that are present within the drusen and in the subretinal space can be synthesized by RPE cells, although some of the proteins may be derived from the choroidal circulation. Therefore, it is highly likely that the RPE cells regulate the activation of the complement pathway and maintain this aspect of retinal homeostasis under physiological conditions. However, once the RPE cells become senescent or pathological, the regulation of the complement pathway might be disturbed.

Although recent genetic studies suggested an important role of the complement system for the pathogenesis of AMD (12–17, 20–23), we suspect that this is probably due to the tissue specificity of the macular area in the eye. The retina is shielded from the plasma components by a blood-tissue barrier like the brain, and furthermore, the retina of the macular area is completely avascular. In such kind of shielded tissue, once unregulated complement activation induced by the accumulated Aβ occurs, it might be difficult to stop the amplification loop. Subsequently, the chronic exposure of RPE cells to bioactive fragments of complement components might induce pathological damage on RPE cells. In addition, chronic activation of complement might cause a migration of monocytes that might be involved in the degradation of Bruch's membrane.

Chronic inflammation induced by complement activation is also considered to be a significant contributor to the neurodegenerative processes in the brains of patients with AD (35, 36, 43, 50, 51). In any case, the pathogenesis of AD and AMD may have many similarities, and the observations made in our study might also apply to the brain of AD patients.

For AMD to develop, an interaction between the environment and genetic susceptibility has been considered to be critical. Very recently, Campochiaro and colleagues demonstrated that oxidative stress reduces the ability of IFN-γ, an inflammatory cytokine, to increase the expression of factor H in RPE cells (52). Also, in an investigation of a potential trigger for complement activation in AMD, Zhou et al. (53) explored the idea that the complex mixture of products resulting from photo-oxidation of A2E might include a range of fragments that could be recognized by the complement system as "foreign," and could activate the complement system, leading to low-grade inflammation. A2E is a bis-retinoid pigment which accumulates as lipofuscin in RPE. They found that iC3b and C3a were elevated in the medium overlying ARPE-19 cells that had accumulated A2E and were irradiated to induce A2E photo-oxidation. In our study, we showed that Aβ directly inactivated factor I. Taken together (52, 53), these data suggest that there are important interactions between environmental exposures and genetic susceptibilities in the pathogenesis of AMD.

In conclusion, we have demonstrated that Aβ binds to factor I and blocks its ability to inhibit the inactivation of C3b, resulting in unregulated complement activation. Our findings provide new insights into the pathogenesis and the treatment strategies of AMD, especially to prevent the progression to AMD from its earliest clinical hallmark of drusen deposits.

Acknowledgments

We thank Prof. Duco Hamasaki for critical discussion and revision of the final manuscript. We also thank Prof. Peter A. Campochiaro and Sean F. Hackett for human RPE cells. We thank M. Sekiguchi, K. Watanabe, and R. Fujioka (RIKEN Brain Institute) for technical assistance.

Disclosures

The authors have no financial conflict of interest.

References

1. Gasque, P. 2004. Complement: a unique innate immune sensor for danger signals. *Mol. Immunol.* 41: 1089–1098.
2. Mayer, M. 1973. The complement system. *Sci. Am.* 229: 54–66.
3. Barnum, S. 1995. Complement biosynthesis in the central nervous system. *Crit. Rev. Oral Biol. Med.* 6: 132–146.
4. Sommer, A., J. M. Tielsch, J. Katz, H. A. Quigley, J. D. Gottsch, J. C. Javitt, J. F. Martone, R. M. Royall, K. A. Witt, and S. Ezrine. 1991. Racial differences in the cause-specific prevalence of blindness in east Baltimore. *N. Engl. J. Med.* 325: 1412–1417.
5. Attebo, K., P. Mitchell, and W. Smith. 1996. Visual acuity and the causes of visual loss in Australia. The Blue Mountains Eye Study. *Ophthalmology* 103: 357–364.
6. VanNewkirk, M. R., L. Weih, C. A. McCrty, and H. R. Taylor. 2001. Cause-specific prevalence of bilateral impairment in Victoria, Australia: the Visual Impairment Project. *Ophthalmology* 108: 960–967.
7. Oshima, Y., T. Ishibashi, T. Murata, Y. Tahara, Y. Kiyohara, and T. Kubota. 2001. Prevalence of age-related maculopathy in a representative Japanese population: the Hisayama study. *Br. J. Ophthalmol.* 85: 1153–1157.
8. Johnson, L. V., W. P. Leitner, M. K. Staples, and D. H. Anderson. 2001. Complement activation and inflammatory processes in drusen formation and age related macular degeneration. *Exp. Eye Res.* 73: 887–896.
9. Ambati, J., A. Anand, S. Fernandez, E. Sakurai, B. C. Lynn, W. A. Kuziel, B. J. Rollins, and B. K. Ambati. 2003. An animal model of age-related macular degeneration in senescent Ccl-2- or Ccr-2-deficient mice. *Nat. Med.* 9: 1390–1397.
10. Hageman, G. S., P. J. Luthert, N. H. V. Chong, L. V. Johnson, D. H. Anderson, and R. F. Mullins. 2001. An integrated hypothesis that considers drusen as biomarkers of immune-mediated processes at the RPE-Bruch's membrane interface in aging and age-related macular degeneration. *Prog. Retin. Eye Res.* 20: 705–732.
11. Nozaki, M., B. J. Raisler, E. Sakurai, J. V. Sarma, S. R. Barnum, J. D. Lambris, Y. Chen, K. Zhang, B. K. Ambati, J. Z. Baffi, and J. Ambati. 2006. Drusen complement components C3a and C5a promote choroidal neovascularization. *Proc. Natl. Acad. Sci. USA* 103: 2328–2333.
12. Klein, R. J., C. Zeiss, E. Y. Chew, J. Y. Tsai, R. S. Sackler, C. Haynes, A. K. Henning, J. P. SanGiovanni, S. M. Mane, S. T. Mayne, et al. 2005. Complement factor H polymorphism in age-related macular degeneration. *Science* 308: 385–389.
13. Edwards, A. O., R. Ritter, K. J. Abel, A. Manning, C. Panhuysen, and L. A. Farrer. 2005. Complement factor H polymorphism and age-related macular degeneration. *Science* 308: 421–424.
14. Haines, J. L., M. A. Hauser, S. Schmidt, W. K. Scott, L. M. Olson, P. Gallins, K. L. Spencer, S. Y. Kwan, M. Noureddine, J. R. Gilbert, et al. 2005. Complement factor H variant increases the risk of age-related macular degeneration. *Science* 308: 419–421.
15. Hageman, G. S., D. H. Anderson, L. V. Johnson, L. S. Hancox, A. J. Taiber, L. I. Hardisty, J. L. Hageman, H. A. Stockman, J. D. Borchardt, K. M. Gehrs, et al. 2005. A common haplotype in the complement regulatory gene factor H (HF1/CFH) predisposes individuals to age-related macular degeneration. *Proc. Natl. Acad. Sci. USA* 102: 7227–7232.
16. Gold, B., J. B. Merriam, J. Zernant, L. S. Hancox, A. J. Taiber, K. Gehrs, K. Cramer, J. Neel, J. Bergeron, G. R. Barile, et al. 2006. Variation in factor B (BF) and complement component 2 (C2) genes is associated with age-related macular degeneration. *Nat. Genet.* 38: 458–462.
17. Maller, J., S. George, S. Purcell, J. Fagerness, D. Altshuler, M. J. Daly, and J. M. Seddon. 2006. Common variation in three genes, including a noncoding variant in CFH, strongly influences risk of age-related macular degeneration. *Nat. Genet.* 38: 1055–1059.
18. Whaley, K., and S. Ruddy. 1976. Modulation of the alternative complement pathways by β1 H globulin. *J. Exp. Med.* 144: 1147–1163.
19. Weiler, J. M., M. R. Daha, K. F. Austen, and D. T. Fearon. 1976. Control of the amplification convertase of complement by the plasma protein β1 H. *Proc. Natl. Acad. Sci. USA* 73: 3268–3272.
20. Jakobsdottir, J., Y. P. Conley, D. E. Weeks, T. S. Mah, R. E. Ferrell, and M. B. Gorin. 2005. Susceptibility genes for age-related maculopathy on chromosome 10q26. *Am. J. Hum. Genet.* 77: 389–407.
21. Dewan, A., M. Liu, S. Hartman, S. S. Zhang, D. T. Liu, C. Zhao, P. O. Tam, W. M. Chan, D. S. Lam, M. Snyder, et al. 2006. HTRA1 promoter polymorphism in wet age-related macular degeneration. *Science* 314: 989–992.
22. Yang, Z., N. J. Camp, H. Sun, Z. Tong, D. Gibbs, D. J. Cameron, H. Chen, Y. Zhao, E. Pearson, X. Li, et al. 2006. A variant of the *HTRA1* gene increases susceptibility of age-related macular degeneration. *Science* 314: 992–993.
23. Yates, J. R. W., T. Sepp, B. K. Matharu, J. C. Khan, D. A. Thurlby, H. Shahid, D. G. Clayton, C. Hayward, J. Morgan, A. F. Wright, et al. 2007. Complement C3 variant and the risk of age-related macular degeneration. *N. Engl. J. Med.* 357: 19–27.
24. Mullins, R. F., S. R. Russell, D. H. Anderson, and G. S. Hageman. 2000. Drusen associated with aging and age-related macular degeneration contain proteins common to extracellular deposits associated with atherosclerosis, elastosis, amyloidosis, and dense deposit disease. *FASEB J.* 14: 835–846.
25. Bora, N. S., S. Kaliappan, P. Jha, Q. Xu, J. H. Sohn, D. B. Dhaulakhandi, H. J. Kaplan, and P. S. Bora. 2006. Complement activation via alternative pathway is critical in the development of laser-induced choroidal neovascularization: role of factor B and factor H. *J. Immunol.* 117: 1872–1878.
26. Green, R. G., and J. B. Harlan. 1999. Histopathologic features. In *Age-Related Macular Degeneration.* J. W. Berger, S. L. Fine, and M. G. Maguire, eds. Mosby, St. Louis, pp. 81–154.
27. Bressler, S. B., M. G. Maguire, N. M. Bressler, and S. L. Fione. 1990. Relationship of drusen and abnormalities of the retinal pigment epithelium to the prognosis of neovascular macular degeneration. The Macular Photocoagulation Study Group. *Arch. Ophthalmol.* 108: 1442–1447.
28. Mukesh, B. N., P. N. Dimitrov, S. Leikin, J. J. Wang, P. Mitchel, C. A. McCarty, and H. R. Taylor. 2004. Five-year incidence of age-related maculopathy: the Visual Impairment Project. *Ophthalmology* 111: 1176–1182.
29. Johnson, L. V., W. P. Leitner, A. J. Rivest, M. K. Staples, M. J. Radeke, and D. H. Anderson. 2002. The Alzheimer's Aβ-peptide is deposited at sites of complement activation in pathologic deposits associated with aging and age-related macular degeneration. *Proc. Natl. Acad. Sci. USA* 99: 11830–11835.
30. Crabb, J. W., M. Miyagi, X. Gu, K. Shadrach, K. A. West, H. Sakaguchi, M. Kamei, A. Hasan, L. Yan, M. E. Rayborn, et al. 2002. Drusen proteome analysis: an approach to the etiology of age-related macular degeneration. *Proc. Natl. Acad. Sci. USA* 99: 14682–14687.
31. Yoshida, T., K. Ohno-Matsui, S. Ichinose, T. Sato, N. Iwata, T. C. Saido, T. Hisatomi, M. Mochizuki, and I. Morita. 2005. The potential role of amyloid β in the pathogenesis of age-related macular degeneration. *J. Clin. Invest.* 115: 2793–2800.
32. Vassar, R., B. D. Bennet, S. Babu-Khan, S. Kahn, E. A. Mendiaz, P. Denis, D. B. Teplow, S. Ross, P. Amarante, R. Loeloff, et al. 1999. β-secretase cleavage of Alzheimer's amyloid precursor protein by the transmembrane aspartic protease BACE. *Science* 286: 735–741.
33. Takasugi, N., T. Tomita, I. Hayashi, M. Tsuruoka, M. Niimura, Y. Takahashi, G. Thinakaran, and T. Iwatsubo. 2003. The role of presenilin cofactors in the γ-secretase complex. *Nature* 422: 438–441.
34. Haass, C., and D. J. Selkoe. 2007. Soluble protein oligomers in neurodegeneration: lessons from the Alzheimer's amyloid-β peptide. *Nat. Mol. Cell Biol.* 8: 101–112.
35. Akiyama, S., S. Barger, S. Barnum, B. Bradt, J. Bauer, G. M. Cole, N. R. Cooper, P. Eikelenboom, M. Emmerling, B. L. Fiebich, et al. 2000. Inflammation and Alzheimer's disease. *Neurobiol. Aging* 21: 383–421.
36. Bradt, B. M., W. P. Kolb, and N. R. Cooper. 1998. Complement-dependent proinflammatory properties of the Alzheimer's disease β-peptide. *J. Exp. Med.* 188: 431–438.
37. Ohno-Matsui, K., I. Morita, J. Tombran-Tink, D. Mrazek, M. Onodera, T. Uetama, M. Hayano, S. I. Murota, and M. Mochizuki. 2001. Novel mechanism

for age-related macular degeneration: an equilibrium shift between the angiogenesis factors VEGF and PEDF. *J. Cell. Physiol.* 189: 323–333.
38. Campochiaro, P. A., and S. F. Hackett. 1993. Corneal endothelial cell matrix promotes expression of differentiated features of retinal pigment epithelial cells: implication of laminin and basic fibroblast growth factor as active components. *Exp. Eye Res.* 57: 539–547.
39. Hellwage, J., S. Kuhn, and P. F. Zipfel. 1997. The human complement regulatory factor-H-like protein 1, which represents a truncated form of factor H, displays cell-attachment activity. *Biochem. J.* 326: 321–327.
40. Klegris, A., C. J. Bissonnette, K. Dorovini-Zis, and P. L. McGeer. 2000. Expression of complement messenger RNAs by human endothelial cells. *Brain Res.* 871: 1–6.
41. Friese, M. A., T. Manuelian, S. Junnikkala, J. Hellwage, S. Meri, H. H. Peter, D. L. Gordon, H. Eibel, and P. F. Zipfel. 2003. Release of endogenous anti-inflammatory complement regulators FHL-1 and factor H protects synovial fibroblasts during rheumatoid arthritis. *Clin. Exp. Immunol.* 132: 485–495.
42. Pasch, M. C., N. H. A. van den Bosch, M. R. Daha, J. D. Bos, and S. S. Asghar. 2000. Synthesis of complement components C3 and factor B in human keratinocytes is differentially regulated by cytokines. *J. Invest. Dermatol.* 114: 78–82.
43. Strohmeyer, R., Y. Shen, and J. Rogers. 2000. Detection of complement alternative pathway mRNA and proteins in the Alzheimer's disease brain. *Mol. Brain Res.* 81: 7–18.
44. Kai, S., T. Fujita, I. Gigli, and V. Nussenzweig. 1980. Mouse C3b/C4b inactivator: purification and properties. *J. Immunol.* 125: 2409–2415.
45. Sahu, A., S. N. Isaacs, A. M. Soulika, and J. D. Lambris. 1998. Interaction of vaccinia virus complement control protein with human complement proteins: factor I-mediated degradation of C3b to iC3b$_1$ inactivates the alternative complement pathway. *J. Immunol.* 160: 5596–5604.
46. Tsiftsoglou, S. A., A. C. Willis, P. Li, X. Chen, D. A. Mitchell, Z. Rao, and R. B. Sim. 2005. The catalytically active serine protease domain of human complement factor I. *Biochemistry* 44: 6239–6249.
47. Nilsson, B., and K. N. Ekdahl. 1998. Components of the alternative pathway. In *The Complement System.* K. Rother, G. O. Till, and G. M. Hansch, eds. Springer, New York, pp. 23–49.
48. Strohmeyer, R., M. Ramirez, G. J. Cole, K. Mueller, and J. Rogers. 2002. Association of factor H of the alternative pathway of complement with agrin and complement receptor 3 in the Alzheimer's disease brain. *J. Neuroimmunol.* 131: 135–146.
49. Chen, M., V. John, and H. Xu. 2006. Synthesis of complement factor H by retinal pigment epithelial cells is down-regulated by oxidized photoreceptor outer segments. *Exp. Eye Res.* 84: 635–645.
50. Rogers, J., N. R. Cooper, S. Webster, J. Schultz, P. L. McGeer, S. D. Styren, W. H. Civin, L. Brachova, B. Bradt, P. Ward, and I. Lieberburg. 1992. Complement activation by β-amyloid in Alzheimer disease. *Proc. Natl. Acad. Sci. USA* 89: 10016–10020.
51. Webster, S., L. F. Lue, L. Brachova, A. J. Tenner, P. L. McGeer, K. Terai, D. G. Walker, B. Bradt, N. R. Cooper, and J. Rogers. 1997. Molecular and cellular characterization of the membrane attack complex, C5b-9, in Alzheimer's disease. *Neurobiol. Aging* 18: 415–421.
52. Wu, Z., T. W. Lauer, A. Sick, S. F. Hackett, and P. A. Campochiaro. 2007. Oxidative stress modulates complement factor H expression in retinal pigmented epithelial cells by acetylation of FOXO3. *J. Biol. Chem.* 282: 22414–22425.
53. Zhou, L., Y. P. Jang, S. R. Kim, and J. R. Sparrow. 2006. Complement activation by photooxidation products of A2E, a lipofuscin constituent of the retinal pigment epithelium. *Proc. Natl. Acad. Sci. USA* 103: 16182–16187.

BRAIN RESEARCH 1216 (2008) 92–103

available at www.sciencedirect.com

ScienceDirect

www.elsevier.com/locate/brainres

BRAIN RESEARCH

Research Report

Females exhibit more extensive amyloid, but not tau, pathology in an Alzheimer transgenic model

Chiho Hirata-Fukae[a], Hui-Fang Li[a], Hyang-Sook Hoe[a], Audrey J. Gray[a], S. Sakura Minami[a,b], Katsuyoshi Hamada[c], Takako Niikura[a], Fang Hua[a], Hiroe Tsukagoshi-Nagai[c], Yuko Horikoshi-Sakuraba[c], Mohamed Mughal[d], G. William Rebeck[b], Frank M. LaFerla[e], Mark P. Mattson[d], Nobuhisa Iwata[f], Takaomi C. Saido[f], William L. Klein[g], Karen E. Duff[h], Paul S. Aisen[a,i], Yasuji Matsuoka[a,j,]*

[a]*Department of Neurology, Georgetown University Medical Center, Washington, DC 20057, USA*
[b]*Department of Neuroscience, Georgetown University Medical Center, Washington, DC 20057, USA*
[c]*Immuno-Biological Laboratories, Takasaki, Gunma 370-0831, Japan*
[d]*Laboratory of Neurosciences, National Institute on Aging Intramural Research Program, Baltimore, MD 21224, USA*
[e]*Department of Neurobiology and Behavior, University of California, Irvine, CA 92697, USA*
[f]*Laboratory for Proteolytic Neuroscience, RIKEN Brain Science Institute, Saitama 351-0198, Japan*
[g]*Cognitive Neurology and Alzheimer's Disease Center, Northwestern University Institute for Neuroscience, Chicago, IL 60208, USA*
[h]*Taub Institute for Alzheimer's Disease Research, Columbia University, New York, NY 10032, USA*
[i]*Alzheimer's Disease Cooperative Study, Department of Neurosciences, University of California San Diego, School of Medicine, San Diego, CA 92093, USA*
[j]*Neurodegeneration Research, GlaxoSmithkline, Shanghai 201203, China*

ARTICLE INFO

Article history:
Accepted 27 March 2008
Available online 10 April 2008

Keywords:
Alzheimer's disease
Transgenic mice
Amyloid beta
Beta-secretase
Neprilysin
Gender difference
Oligomer
Tau
Hyperphosphorylation

ABSTRACT

Epidemiological studies indicate that women have a higher risk of Alzheimer's disease (AD) even after adjustment for age. Though transgenic mouse models of AD develop AD-related amyloid beta (Abeta) and/or tau pathology, gender differences have not been well documented in these models. In this study, we found that female 3xTg-AD transgenic mice expressing mutant APP, presenilin-1 and tau have significantly more aggressive Abeta pathology. We also found an increase in beta-secretase activity and a reduction of neprilysin in female mice compared to males; this suggests that a combination of increased Abeta production and decreased Abeta degradation may contribute to higher risk of AD in females. In contrast to significantly more aggressive Abeta pathology in females, gender did not affect the levels of phosphorylated tau in 3xTg-AD mice. These results point to the involvement of Abeta pathways in the higher risk of AD in women. In addition to comparison of pathology between genders at 9, 16 and 23 months of age, we examined the progression of Abeta pathology at additional age points; i.e., brain Abeta load, intraneuronal oligomeric Abeta distribution and plaque load, in male 3xTg-AD mice at 3, 6, 9, 12, 16, 20 and 23 months of age.

* *Corresponding author.* Department of Neurology, Georgetown University Medical Center, 4000 Reservoir Road NW, Washington, DC 20057, USA. Fax: +1 202 784 3504. Neurodegeneration Research, GlaxoSmithkline, No.3 Building, 898 Halei Road, Zhangjiang Hi-tech Park, Pudong, Shanghai 201203, China. Fax: +86 21 5895 4331.
E-mail addresses: ym56@georgetown.edu, yasuji.matsuoka@gsk.com (Y. Matsuoka).

doi:10.1016/j.brainres.2008.03.079

These findings confirm progressive Abeta pathology in 3xTg-AD transgenic mice, and provide guidance for their use in therapeutic research.

1. Introduction

Alzheimer's disease (AD) is a neurodegenerative disease that is the most common form of dementia. Only a small portion (< 1%) of cases have known genetic causes, while the majority of AD cases are sporadic (Cummings, 2004). The most significant non-genetic risk factor for AD is age; the risk of AD doubles between the age groups of 65–70 and 70–74. In addition to age, various factors, such as medical history (head injury, stroke, hypertension, hypercholesterolemia, stress, etc.), life style (diet, lack of exercise, alcohol consumption, smoking, etc) and education, may be associated with AD (McDowell, 2001). Epidemiological studies also indicate that women have a higher risk of AD (Brookmeyer et al., 1998) even after adjusting for age (Hy and Keller, 2000). The precise cause of the higher risk of AD in women is unknown.

The pathological hallmarks of AD are amyloid plaques in the extracellular space and intraneuronal neurofibrillary tangles (Hyman, 1997). Amyloid beta (Abeta), the primary component of amyloid plaques, is generated from the amyloid precursor protein (APP) by sequential proteolytic cleavage at the beta and gamma sites (Hardy and Selkoe, 2002). Freshly generated Abeta forms oligomers on and within neurons (Walsh et al., 2000) and compromises hippocampal long-term potentiation in vivo (Walsh et al., 2002). Neurofibrillary tangles are composed of hyperphosphorylated tau, a neuronal microtubule-associated protein. Phosphorylation of tau regulates its ability to promote microtubule assembly (Lindwall and Cole, 1984); hyperphosphorylation interferes with the normal biological functions of tau by reducing its ability to bind to and stabilize microtubules (Trojanowski and Lee, 1995). All genetic mutations that cause familial AD are linked to the Abeta cascade, while tau mutations are associated with AD and several other forms of dementia including frontotemporal dementia and progressive supranuclear palsy (Hardy and Selkoe, 2002). The clinical progression of AD is closely related to tau pathology (Braak and Braak, 1995). In animal models, modulation of Abeta or tau cascades alter pathology and influence cognitive function (Barten et al., 2005; SantaCruz et al., 2005).

To investigate the mechanisms of these pathological events and explore therapeutic strategies, various lines of transgenic mice have been created (McGowan et al., 2006). Overexpression of mutant APP elevates Abeta production leading to plaque formation (Games et al., 1995; Hsiao et al., 1996). Overexpression of mutant presenilin (PS)-1 elevates the level of endogenous Abeta slightly, but does not induce Abeta plaque deposition (Duff et al., 1996). Mice obtained by crossing APP and PS-1 transgenic mice show dramatically accelerated Abeta pathology (Holcomb et al., 1998) associated with oxidative stress and neuroinflammation (Matsuoka et al., 2001a,b). Overexpression of mutant tau causes hyperphosphorylation and tangle formation (Lewis et al., 2000). In many tau transgenic mice, tauopathy is more evident in the brainstem and spinal cord and is associated with motor dysfunction. Some tau transgenic mice, including the one used in this study, show tau pathology in the brain along with cognitive impairment (Ramsden et al., 2005).

Currently available AD mouse models are well-characterized, but the effects of gender on Abeta and tau pathology in animal models have not been carefully examined. Previously, gender differences have been studied in Tg2576 APP transgenic mice, which develop Abeta, but not tau pathology. In that study, female mice showed more histologically-determined Abeta plaques at 15 and 19 months of age and ELISA-quantified Abeta 1–40 (but not Abeta 1–42) load at 15 months of age (Callahan et al., 2001). Mice at these two time points bear Abeta plaques; the effect of gender at the pre-plaque stage was not evaluated. Abeta and tau pathology influence each other, but gender influences on the co-occurrence of these two aspects of AD pathology have not been examined. In this study, we examined the progression of AD-related pathology in male and female mice during the course of their lifespan using transgenic mice which develop both Abeta and tau pathology. In addition, we also investigated the progression of Abeta pathology in male mice at additional age points.

2. Results

2.1. Soluble and total Abeta 1–40 and 1–42 are increased with aging after plaque formation

Our Abeta ELISAs were composed of N and C-terminus end-specific antibodies to quantify full-length Abeta 1–40 and 1–42 (Horikoshi et al., 2004). Both the Abeta 1–40 and 1–42 ELISAs provide linear (r^2>0.99) standard curves over the range of 1–800 fmol/ml (pM). In this study, results from multiple plates needed to be combined; therefore, to assure quality control, we used a higher cut-off, 10 fmol/ml, which is equivalent to 220 and 6500 fmol/g tissue in diethylamine (DEA) and formic acid (FA) fractions, respectively (this cut-off level is indicated by dashed line in Fig. 1). Samples were analyzed using multiple ELISA plates. The variance of the internal reference, pooled human plasma, was within 5% among plates; thus we used values obtained by ELISA assays without adjustment.

DEA-extracted soluble Abeta 1–40 was detectable from 3 months of age, the youngest age we examined in this study, and the level was stable until 12 months of age in male 3xTg-AD mice (Fig. 1A squares). The soluble Abeta 1–40 level began to rise between 12 and 16 months of age in male 3xTg-AD mice, and continued to increase with aging. Abeta plaques were first detected around 14 months of age in male 3xTg-AD mice (Fig. 4E), which is close to when ELISA-detected Abeta 1–42 began to rise. Soluble Abeta 1–42 was below the quality control cut-off until 12 months of age and barely detectable at 16 months of age in male 3xTg-AD mice (Fig. 1A circles). Soluble Abeta 1–40 was much more abundant, >10 fold,

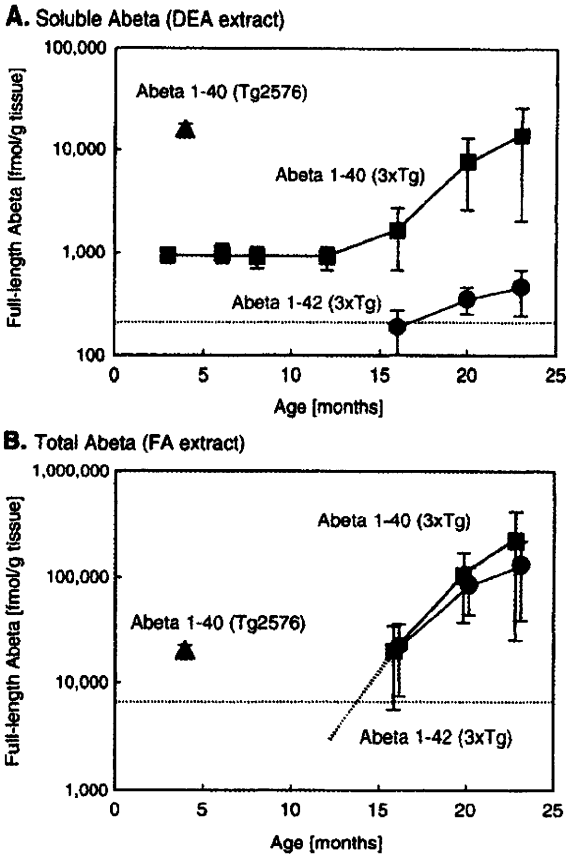

Fig. 1 – Levels of full-length Abeta 1–40 and 1–42 are increased with aging in male 3xTg-AD mice. Levels of DEA-extracted soluble (A) and FA-extracted total (B) Abeta 1–40 and 1–42 were determined in male 3xTg-AD mice ($n=6$ each) and male Tg2576 mice ($n=5$ each). Dashed lines at 220 and 6500 fmol/g tissue in DEA and FA fractions, respectively, indicate the limit of fully-reproducible and reliable Abeta detection (10 fmol Abeta/ml extract, note: the detection limit is 1 fmol/ml extract). FA extraction requires 1:20 neutralization during the sample preparation, and the signals were diluted in young mice. Please note that Y-axis is in log scale.

compared to soluble Abeta 1–42 (Fig. 1A squares vs circles). The commonly used APP single transgenic Tg2576 mice (male) had much higher soluble Abeta 1–40 at 4 months of age (Fig. 1A triangle), but soluble Abeta 1–42 was not detectable. 3xTg-AD mice with a similar level of Abeta 1–40 (>20 months of age) bear Abeta plaques, while Tg2576 mice at 4 months of age are free of any plaque pathology. This suggests that the absolute level of Abeta 1–40 is not a critical factor in Abeta plaque formation.

FA-extracted total Abeta 1–40 and 1–42 were not detectable until 16 months of age in male 3xTg-AD mice, while total Abeta 1–40 was detectable in Tg2576 mice from 3 months of age, the youngest age we examined in this study (Fig. 1B triangle). FA extraction required 1:20 neutralization prior to ELISA analysis, and the neutralization dilutes the signals; thus FA-extracted total Abeta levels were below the cut-off at younger ages. Levels of total Abeta 1–40 and 1–42 were similar and gradually increased with aging (Fig. 1B squares and circles, respectively).

2.2. *Abeta plaques and intraneuronal Abeta increase with aging*

We examined Abeta and APP pathology using two antibodies: 82E1, specific to the N-terminus end of Abeta (epitope: 1–5 amino acids of cleaved Abeta) and not cross-reactive to uncleaved APP, and 6E10, fully cross-reactive to uncleaved APP, soluble APP cleaved at alpha site (sAPPalpha), and Abeta (epitope: 3–8). 82E1-immunostaining was detectable in neurons in the frontal cerebral cortex starting at 6 months of age, and extended to the middle of the brain by 9 months of age (Fig. 2A). Abeta plaques were first observed in the subiculum and then gradually extended to the hippocampus (Fig. 2C). In the hippocampal formation, 82E1 detected plaques as well as some pyramidal neurons weakly (Fig. 2G). Intraneuronal staining was much more intense in the cerebral cortex (Figs. 2G vs H). APP-cross-reactive 6E10 stained neurons in the cerebral cortex and hippocampal CA1 prior to the age at which plaques became detectable (Figs. 2D, E). In addition to intraneuronal staining, 6E10 stained extracellular plaques (Figs. 2F, I). Both 82E1 and 6E10 resulted in similar intraneuronal staining in the cerebral cortex (Figs. 2H, J). In contrast to the cerebral cortex, 82E1 and 6E10 staining in the hippocampal formation were distinct. While uncleaved APP-cross-reactive 6E10 stained pyramidal neurons strongly (Fig. 2I), cleaved Abeta-specific 82E1 detected only a few neurons weakly (Fig. 2G). These results suggest that 6E10 immunostaining in the hippocampal pyramidal neurons is primarily due to its cross-reactivity to uncleaved APP and sAPPalpha.

2.3. *Oligomeric Abeta accumulates inside of neurons in 3xTg-AD mice*

Oligomeric Abeta was examined using an anti-Abeta-derived diffusible ligands (ADDL) antibody, clone NU-1 (Lambert et al., 2007). In 3xTg-AD mice, intraneuronal staining in the cortex of the frontal region was detectable from 6 months of age, and became more evident at 9 months of age (Fig. 3C). Neuronal staining in the cortex in the middle region was less evident compared to the frontal brain (Figs. 3A vs B). A conventional Abeta antibody, 82E1, also detected intraneuronal staining in the cortex (Figs. 2A–C). In addition to the staining in the cortex, NU-1-staining was seen in the intraneuronal space in the subiculum where Abeta plaques first became detectable at 14 months of age (Figs. 3B, D). At older ages, intraneuronal staining became more evident and plaques were also stained by NU-1 antibody (Figs. 3E–I). Some cells surrounding the plaques were also immunostained with NU-1 (Fig. 3H).

We also examined oligomeric Abeta in a different AD transgenic mouse model, PS/APP (Duff et al., 1996). APP transgene expression is under the control of the prion promoter, which drives transgene expression mainly in neuronal cells in PS/APP mice, while it is under the control of neuron-specific Thy-1 promoter in 3xTg-AD mice. In PS/APP mice, Abeta plaques were detectable from 2 months of age (Fig. 3J). At 2 months of age, cells surrounding plaques were not immunopositive with NU-1 (Fig. 3M); with aging, more plaques appeared and cells

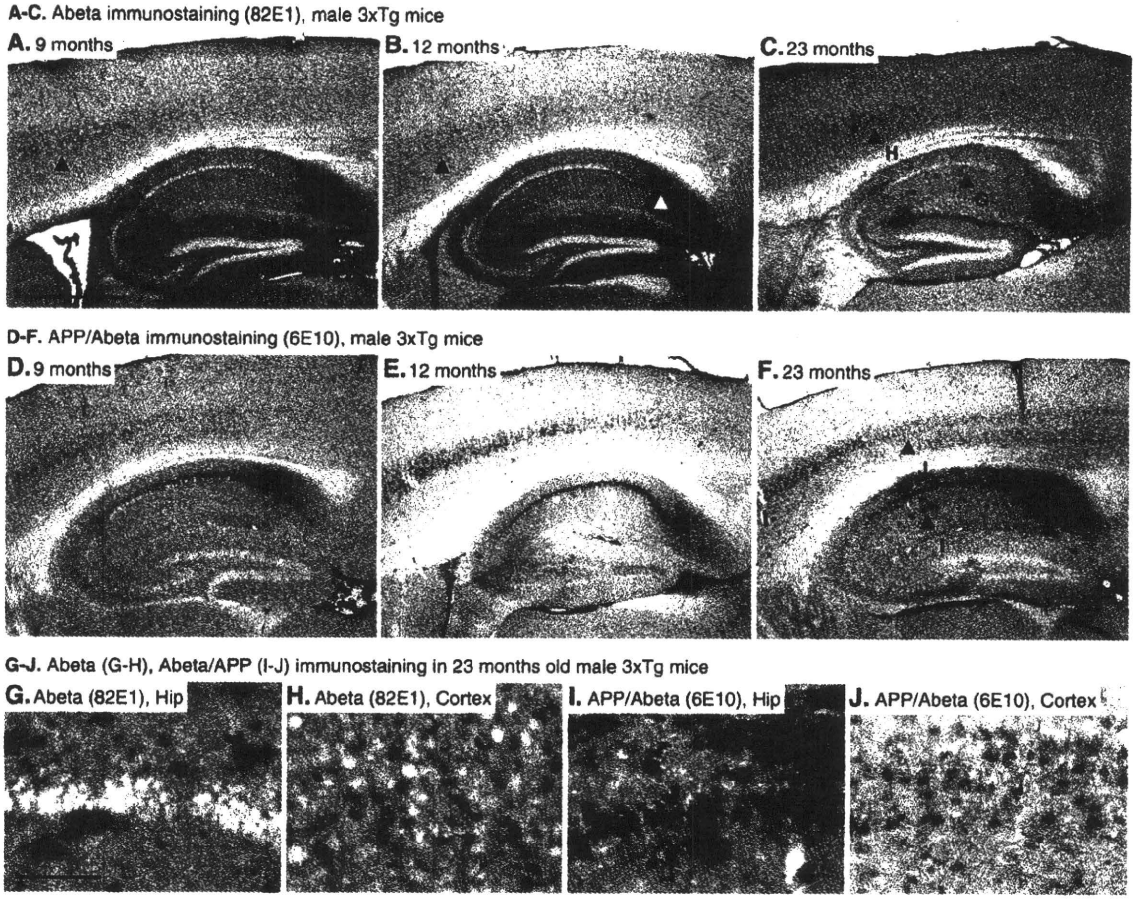

Fig. 2 – Abeta and APP pathology increase with aging. Sagittal sections from male 3xTg-AD mice at 9, 12, 14 and 23 months of age were immunostained with 82E1 antibody (A–C, G, H) or 6E10 antibody (D–F, I, J). 82E1, not cross-reactive with uncleaved APP, detected intraneuronal Abeta in the cerebral cortex of the frontal brain region from 6 months of age, and expanded toward the middle of the brain at 9 and 12 months of age (A, B, indicated by closed arrow heads). At 12 months of age, 82E1 detected intraneuronal staining in the subiculum (B, indicated by open arrow heads). Uncleaved APP and sAPPalpha cross-reactive antibody, 6E10, detected strong intraneuronal staining in wider area; cortex and hippocampal pyramidal neurons (D–F, I. J). Bar=200 μm in A for A–F; 20 μm in G for G–J.

surrounding Abeta plaques became NU-1 immunopositive (Figs. 3N–P). However, intraneuronal Abeta staining was hard to detect in PS/APP mice under the experimental conditions we used. We also used another ADDL antibody, NU-2 (Lambert et al., 2007), for 3xTg-AD and PS/APP mice and obtained similar staining patterns (data not shown).

2.4. *Female mice show more aggressive Abeta pathology than male mice after plaque formation*

We examined gender differences in Abeta load using age-matched male and female mice. Tg2576 mice at 4 months of age and 3xTg-AD mice at 9 months of age are free of Abeta plaques. Levels of soluble Abeta 1–40 were similar between genders (Fig. 4A). FA-extracted total Abeta 1–40 was detectable in Tg2576 mice, and there was no difference between genders (Fig. 4C).

In contrast to the plaque-free stage, there was a significant gender difference in plaque-bearing mice. Levels of soluble Abeta 1–40 and 1–42 in female mice were higher (Abeta 1–40: 461%, $P=0.058$; Abeta 1–42: 175%, $P=0.065$) at 16 months of age (Figs. 4A, B), and the difference became clearer at 23 months (Abeta 1–40: 407%, $P=0.006$; Abeta 1–42: 190%, $P=0.003$). FA-extracted total Abeta levels were significantly higher in female 3xTg-AD mice at 16 (Abeta 1–40: 648%, $P=0.017$; Abeta 1–42: 330%, $P=0.047$) and 23 months of age (Abeta 1–40: 161%, $P=0.003$; Abeta 1–42: 208%, $P=0.011$) (Figs. 4C, D). Histology revealed similar gender differences (see below).

As suggested by the ELISA results, Abeta plaque pathology was more evident in female mice compared to age-matched male mice. At 14 months of age, Abeta plaques were barely detectable in male mice, while several plaques were seen in the subiculum in the female mice (Figs. 4E/F vs G/H).

2.5. *Female mice have higher beta-secretase activity and less efficient Abeta degradation*

It has been suggested that Abeta production and degradation are altered with aging (Hyman, 1997; Iwata et al., 2005). Changes

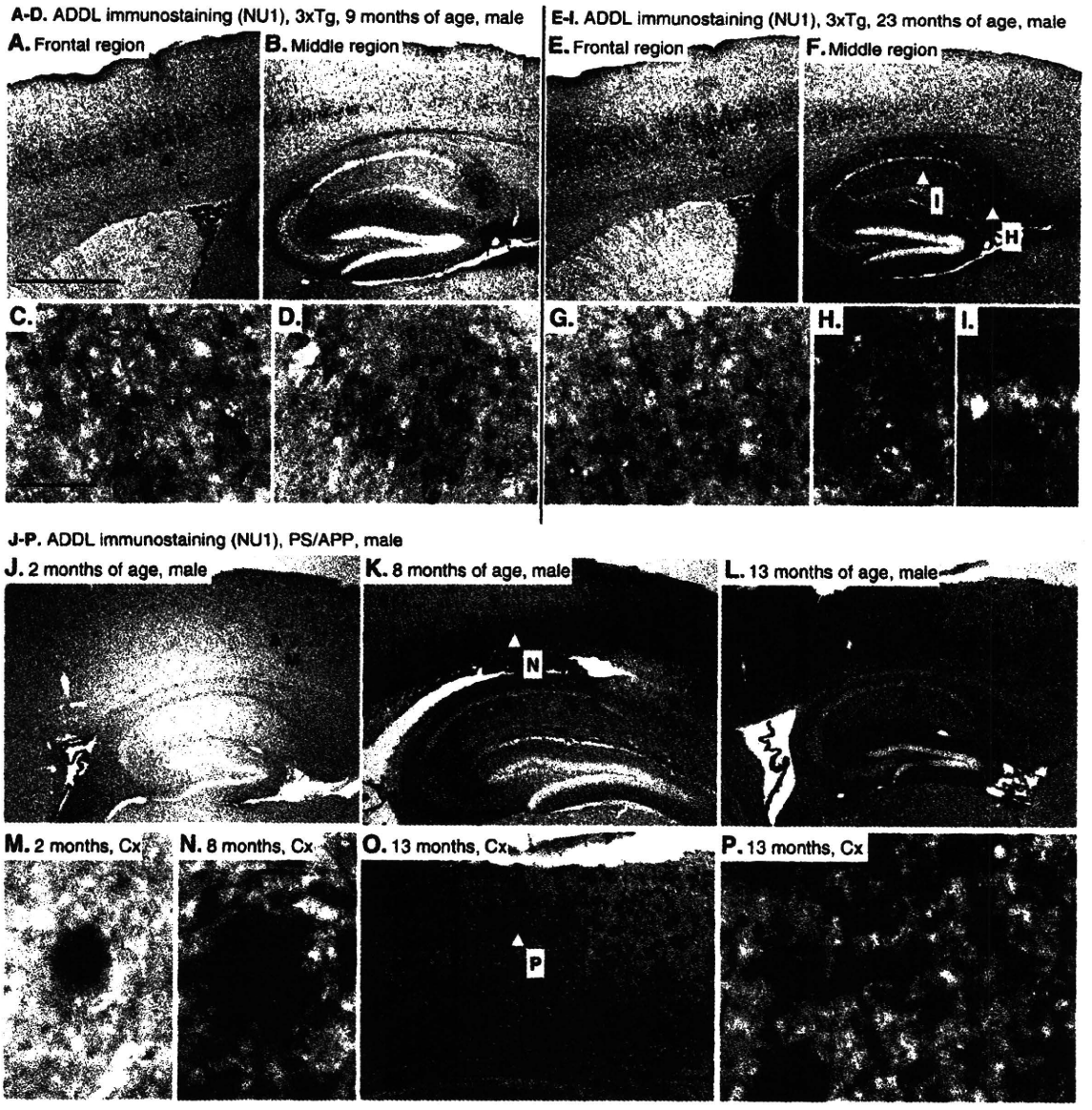

Fig. 3 – Intraneuronal Abeta in 3xTg-AD mice. Sagittal sections from male 3xTg-AD (A–I) and PS/APP (Holcomb et al., 1998) (J–P) mice were immunostained using an anti-ADDL antibody NU-1 (Lambert et al., 2007). NU-1 detected intraneuronal staining in the cortical neurons from 6 months of age in the frontal brain region, and expanded toward the middle of the brain at 9 months of age (A–C). In addition, the intraneuronal, but not the extracellular plaque, staining was detected in the subiculum at 9 months of age (D). At older ages, intraneuronal staining became stronger and the extracellular plaques were also detected (H, I). In PS/APP mice, there is no obvious intraneuronal staining with NU-1 (J–L). At 2 months of age, plaques were stained with NU-1 but there is no cellular staining surrounding the plaques (J, M). At older age, cells surrounding plaques were also ADDL-immunopositive at 8 and 13 months of age (N–P). Bar=200 μm in A for A, B, E, F, J–L; 20 μm in C for C, D, G–I, M, N, P; 100 μm in O for O.

in Abeta production and degradation in 3xTg-AD mice were examined using levels of soluble APP cleaved at the beta site (sAPPbeta) and neprilysin as indicators. A rabbit polyclonal antibody we previously developed (Nishitomi et al., 2006) is specific to wild-type sAPPbeta and not cross-reactive with Swedish mutant sAPPbeta. For the present study, we developed a mouse monoclonal antibody against Swedish-type sAPPbeta, clone 6A1 (Fig. 5B); this antibody did not cross-react with uncleaved Swedish APP or wild-type sAPPbeta (Fig. 5A). Immunocytochemical staining of cells transfected with either wild-type or Swedish mutant APP confirmed the specificity of these antibodies (data not shown).

The level of sAPPbeta was significantly higher in female 3xTg-AD mice compared to male 3xTg-AD mice at 9 months of

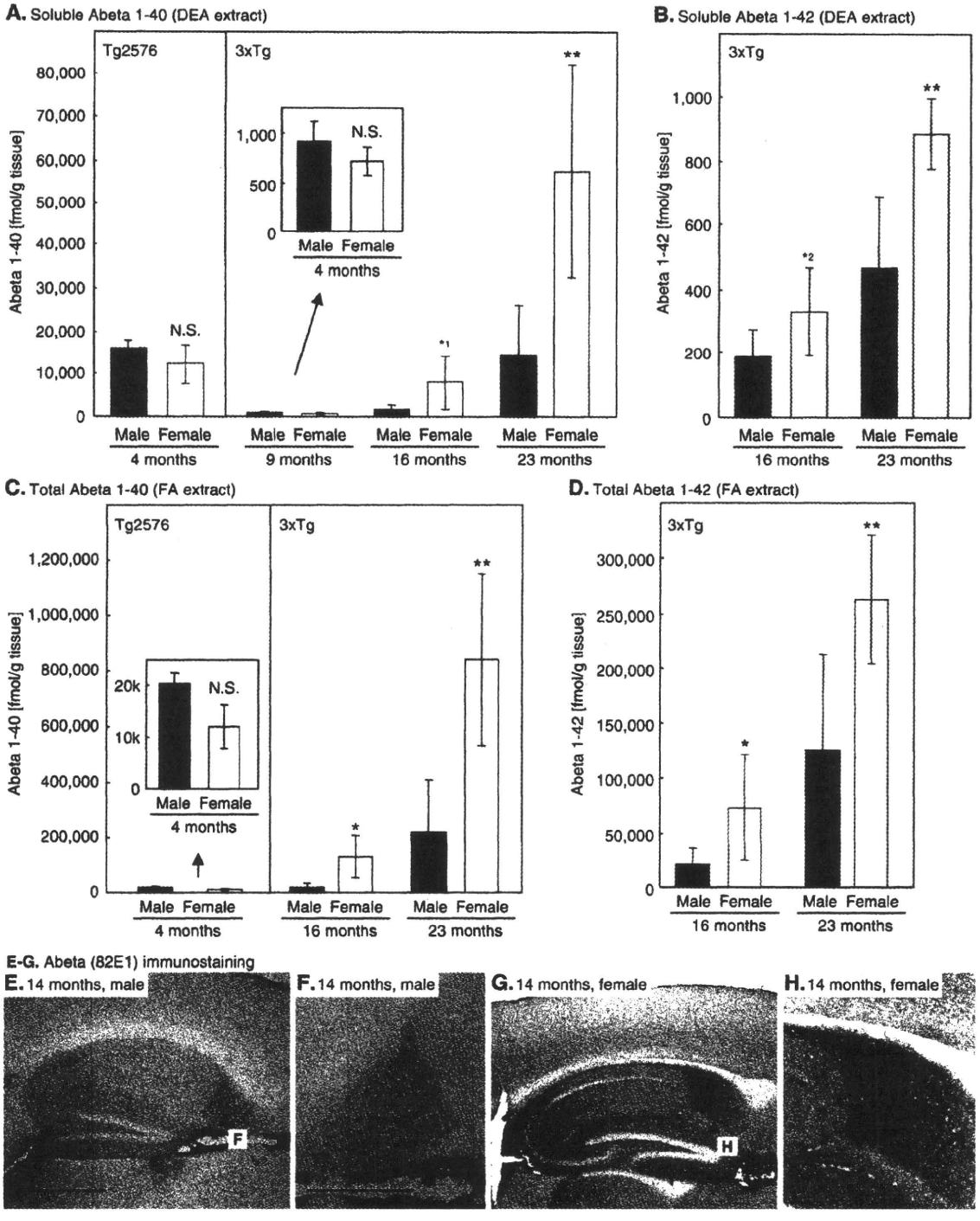

Fig. 4 – Female mice have higher level of soluble and total Abeta in 3xTg-AD. Levels of DEA-extracted soluble and FA-extracted total Abeta 1–40 (A, DEA; C, FA) and 1–42 (B, DEA; D, FA) in each gender were determined in 3xTg-AD mice and Tg2576 mice. 3xTg-AD at 9 months and Tg2576 mice at 4 months of age are free from any plaque pathology. *P<0.05 and **P<0.01 compared with age-matched male mice using t-test. DEA-extracted soluble Abeta 1–40 (A) and 1–42 (B) in mice at 16 months of age showed marginal significance: *1P=0.058 and *2P=0.065. Gender difference was also seen in Abeta plaque pathology. Female mice at 14 months of age have plaques in the subiculum (G, H), while plaques are not evident in male mice (E, F). Bar=200 μm in E for E, G; 100 μm in F for F, H.